

Authors' response to Reviewer 1

Summary and Recommendation

Comment from Referee: In this study, a high-resolution surface-unsaturated zone-aquifer flow model was fit to a km² scale hilly drainage basin near Los Angeles, to investigate spatial and temporal variability of groundwater recharge. The main result is that, although the long-term spatial average recharge under the catchment is 16 mm/yr, under the small alluvial valley after heavy rain, focused temporal recharge rate may reach 1000 mm/yr.

Although this type of variability in recharge is not totally new for this setting, the work is worthy for its rare and intensive modelling effort and comparison with local estimates (e.g. chloride mass balance). Nevertheless, substantial changes need to be made in the manuscript before it can be published in HESS.

Author's response: We thank reviewer 1 for the positive feedback and for recognizing the modeling effort we put in place. We tried to respond exhaustively to all the comments and modify the text accordingly.

Major comments

1) Comment from Referee: Structure: There is no Methods section and no Discussion in the paper. The authors avoiding the classic titles of sections in a scientific paper is deep in the content, many methods are not clear (S. comments 7-10, 13 below), and there is no discussion of the results with the wide literature on recharge. Methods and Discussion sections should be included and taken more seriously (it could be Results and Discussion but a discussion should be done).

Author's response: The description of the methodology used is in the MIKE SHE model section. We expanded this section to make it clearer and more comprehensive, responding to the reviewers' comments.

A discussion about recharge characteristics and about the occurrence of preferential flow in the ET zone has been added to the "conceptual model of recharge" that now has become "Discussion and conceptual model for recharge" section.

Author's changes in manuscript:

Comments 7-10 and 13 were addressed (see response to specific comments below for details about changes in the manuscript).

Text added to the discussion section:

- Line 520 – 523: The average recharge value is 16 mm y^{-1} which is consistent with previous estimates at the site, and with those obtained for other sandstone aquifers in semi-arid areas in the United States (4% - Heilweil et al., 2006) and other studies in semi-arid regions around the world ($0.2 – 35 \text{ mm y}^{-1}$ equal to 0 – 5% of the average precipitation, Scanlon et al., 2006).
- Line 529-535: Generally, in semiarid regions, high recharge values along a valley, at the edge of the slope referred to as Mountain Front Recharge (MFR) (Wilson and Guan, 2004). However, our catchment is located on the top of a ridge standing 300 m above the surrounding valleys (Manna et al., 2016) and, thus, our case study represents groundwater recharge on the mountain block rather than MFR. Nonetheless, it is interesting that the processes observed in our small catchment are similar to those described for aquifer-scale recharge studies (Aishlin and McNamara, 2011; Carling et al., 2012; Manning and Solomon, 2003; Bresciani et al., 2018) and defined as MFR.
- Line 550-556: Case studies showing similar results for water that crosses the ET zone preferentially in time and space to become potentially recharge have been also reported in literature (Kurtzman et al., 2016), also referred to as selective recharge (Gat and Tzur, 1967; Florea, 2013; Krabbenhoft et al., 1990) . The occurrence of these fluxes has been also analyzed in function of precipitation characteristics and antecedent water content with rainfall intensity being the main factor (Allocca et al., 2015; Crosbie et al., 2012; Nasta et al., 2018; Taylor et al., 2013).

2) Comment from Referee: Concerning the discussion above: I would say that the recharge characteristics described in the manuscript is similar to what many studies term: Mountain Front Recharge (MFR). Aquifers under alluvial valleys in mountainous regions are recharged from the edge of the valley (mountain front) or maybe altogether in subsurface recharge of rain percolating in the mountain block (can explain fresh groundwater above saline unsaturated zone). Discuss your findings in light of MFR literature.

Author's response: We thank you the reviewer for this suggestion that allowed us to describe better our conceptual model and the hydrologic processes involved. The spatial distribution of recharge and the proposed conceptual model might recall what has been defined Mountain Front Recharge (Wilson and Guan, 2004). However, the catchment is located on an upland ridge that represents, on a regional scale, the mountain block. Although the processes observed are similar to those described as diffuse and focused MFR (direct water-table recharge at the edge of a slope front), we believe that recharge characteristics are more similar to recharge at the mountain block. A classic MFR and MBR approach would have been more plausible at regional scale, perhaps including the surrounding Simi and San Fernando valleys (about 300 m below the studied catchment). Instead, we only focused on a small watershed (2.16 km^2), with a local relief of 150 m located on the top of the Simi Hills. The maximum thickness of the alluvium overlying the sandstone bedrock in the low areas of the catchment, where the majority of recharge occurs, is only 3.8 m and therefore this setting is different from the alluvial-filled basins described in several Mountain Front recharge papers (Aishlin and McNamara, 2011; Carling et al., 2012; Manning and Solomon, 2003; Bresciani et al., 2018). Given all these considerations, we believe

that the system represents a small portion of the Mountain Block rather than the MFR (see Figure 1 at the end of the document) although, by analogy to much different scale, we add reference to these concepts in our discussion.

The presence of less saline groundwater below a more saline vadose zone in our case has been attributed by Manna et al. (2017) to preferential flow along the fracture network in the vadose zone. This fast component of the unsaturated flow represents, on average, only 20% of the total recharge with the majority of the flow occurring in the porous matrix blocks.

Author's changes in manuscript: We added some text with reference to MFR in the discussion and conceptual model (see comment 1)

3) Comment from Referee: Figures graphics. Although digital era, some of us do print and read from paper some of their work (manuscripts for review, especially). The manuscript include figures with axis-titles that are extremely small (unreadable). Check figures graphics on a printed version with a reader older than 50.

Author's response: We increased the size of the fonts to improve the readability.

Specific comments

1) Comment from Referee: L25 The Abstract is a standalone entity, it should not contain references.

Author's response: Accepted. We removed references from the abstract

2) Comment from Referee: L49 and throughout the manuscript – put a space after the semicolon.

Author's response: Accepted. We modified throughout the manuscript.

3) Comment from Referee: L62 I would change “transient” to fast changing. The literature is full of examples of changing recharge due to change in land-use that were shown via chloride mass balance and similar methods.

Author's response: We changed to “dynamic, short-term” temporal effects

4) Comment from Referee: L64-L70. In many semiarid regions surface run-off is ~1% of precipitation way within the modeling error, hence sub-surface unsaturated - saturated zone flow models (and in some cases even only unsaturated zone models) are a very reasonable choice for studying recharge and contamination. This type of studies are quite common in the literature of the last decade (e.g. Levi et al.,

2017 HESS; Turkeltaub et al., 2015 WRR). Therefore, the elaboration on 2006 review, is outdated and not very convincing, I suggest to discard.

Author's response:

Embracing the reviewer's suggestion, we added more recent references of recharge studies in semi-arid environments using different approaches. The elaboration on Scanlon et al., 2006 was introduced to show that until that date only few modeling studies were carried out in semiarid regions, mainly at the regional scale. We left the reference to the main paper and discarded the citations of the single studies. Anyway, we would like to highlight the lack of papers that feature an integrated surface water and groundwater approach in semiarid environments. Sometime, as the reviewer pointed out, this interaction can be considered negligible but, in several cases (like the presented manuscript), it has a huge impact on the spatial distribution of recharge.

Author's changes in manuscript: line 64-76. Text added.

Numerical hydrologic models that integrate surface water and groundwater flows have been developed to simulate the spatial and temporal distribution of surface runoff, infiltration, evapotranspiration and groundwater recharge. However, the application of nearly all such simulation tools have been limited to humid regions (Wheater et al., 2007) with minimal application to semiarid regions. Scanlon et al. (2006), in their review on recharge in semiarid areas, reported only 7 papers providing a continuous spatial distribution of recharge, out of a total of 98 studies. However, these studies investigated large areas, from 1,039,647 km² (Flint and Flint, 2007) to 60 km² (Flint et al., 2001), using a relatively coarse spatial resolution (from 72,900 m² - Flint and Flint, 2007 to 900 m² - Flint et al., 2001). In the last decade, although modeling techniques have advanced to include combined surface water-groundwater simulations, recharge in semiarid areas has been represented with a GIS approach (Hernández-Marín et al., 2018) often using remote sensing data (Wang et al., 2008; Coelho et al., 2017; Crosbie et al., 2015) or neglecting the surface water component and focusing on unsaturated zone (Levy et al., 2017; Turkeltaub et al., 2015).

5) Comment from Referee: L88. Potential evaporation – give the numbers.

Author's response: 1400 mm y⁻¹. Added to the text.

6) Comment from Referee: L 93 chemical contamination – say what contamination (in 2-3 words, nitrate, industrial organic compounds).

Author's response: The main contaminant is Trichloroethene (TCE). Added to the text.

7) Comment from Referee: L140 – How is infiltration capacity modeled? is it constant at field capacity or starts significantly higher after a dry period?

Author's response: Infiltration capacity of soil in the model is dynamic and a function of the conductivity of the surficial material and the water content properties (saturation point, field capacity and wilting point). The conductivity of the soils is a function of degree of saturation in the soil and a soil moisture

characteristic curves. The soil moisture characteristic curve describes the variation in soil water content and conductivity and matric potential. The Van Genuchten model is used to describe the soil moisture characteristic curves in this MIKE SHE model. The conductivity and matric potential of subsurface materials is computed for each layer within the unsaturated zone at each time step. Values used have been added to table 2 for more clarity.

Author's changes in manuscript: line 148-152. Text added: The infiltration capacity in the model is dynamic and a function of the unsaturated hydraulic conductivity (K_u) and the water content properties (i.e., saturation point, field capacity and permanent wilting point) of the surficial media. To describe the relation between water content, conductivity and matric potential, the Van Genuchten model is used (Van Genuchten, 1980)

8) Comment from Referee: L143-146 – Not clear is the root zone and the deeper unsaturated zone modeled as a continuous domain with Richards Equation with root water uptake sink at the root zone. Or is the root-zone modeled as bimodal: above FC –deep drainage, below no deep drainage?

“...It is mainly vertical” is it a 1D model in this zone, or of higher dimension.

Author's response: The unsaturated zone is a continuous domain that is modelled as a 1D column of finite difference cells which have variable discretization from the top of the column (ground surface) to the base of the column (the unsaturated/saturated zone interface). The Richard's equation governs flow throughout the unsaturated zone. Typically, when we refer to the root zone we are describing that portion of the unsaturated zone in which vegetation has roots and the capillary fringe which may exist below the roots themselves.

Author's changes in manuscript: Line 155-159. Text added: The unsaturated zone flow is simulated as the change in soil moisture, resulting from cyclical input (infiltration) and output (recharge and evapotranspiration). It is modelled as a 1D column using the full Richards equations (Richards, 1931) with finite difference cells that have variable discretization from the top of the column (ground surface) to the base of the column (the unsaturated/saturated zone interface).

9) Comment from Referee: L153-154, as far as I understand if there is a constant head as a bottom boundary condition the water table will not change and recharge or discharge will be reflected only by flux out or into the model domain. Was the model fitted to transient head in wells? or only to a steady-state approximation? If so, say it explicitly in Figure 6 captions.

Author's response: There is a fixed head boundary conditions applied to the base of the model based on observed groundwater levels. If heads in the layer above the base layer of the model exceed the fixed heads then water will flow out of the model, conversely if heads in the layer above the base layer of the model fall below those in the fixed head then water will flow into the model. The model was calibrated to long term average groundwater levels over the period of simulation (1995-2014).

Author's changes in manuscript. Line 166 – 174. Text added: A fixed head boundary applied along the lateral sides and the bottom of the model domain (490 m asl) was used to simulate the flow to and from the deeper groundwater system, not explicitly represented in the integrated model but which extends

several hundred meters (Fig. 3). These fixed heads are based on observed groundwater levels at the site and simulations based on a detailed 3-D groundwater flow model system that includes the catchment and a much larger domain beyond (AquaResource and MWH, 2007). The groundwater contribution to streamflow is minimal and intermittent ($\sim 0.1 \text{ mm y}^{-1}$ for the period of 1995-2014) and only occurs at the farthest downstream location of the catchment where the groundwater table rises close to the ground surface.

10) Comment from Referee: L187 – “physical properties” there is only Ks in the table (not enough to model unsaturated zone flow, parameters of hydraulic functions? What type of functions? – not clear

Author’s response: The table has been completed with porosity, field capacity, residual water content and the Van Genuchten parameters (α , n) used in the model.

Hydrogeologic unit	$K_s \text{ (m s}^{-1}\text{)}$	Saturation (θ_s)	Field capacity (θ_{fc})	Residual Water content (θ_{rc})	Van Genuchten parameters		
					α	n	l
Alluvium	1×10^{-6}	0.4	0.25	0.05	0.021	1.61	0.5
Weathered bedrock	2×10^{-7}	0.2	0.11	0.01	0.033	1.49	0.5
Unweathered bedrock	4.1×10^{-10} to 2.3×10^{-7}	0.13	0.1	0.025	0.01	1.23	0.5
Unweathered bedrock	1×10^{-10} to 1×10^{-5}	0.13	0.09	0.01	0.01	2	0.5
Unweathered bedrock	1×10^{-9} to 1×10^{-6}	0.13	0.1	0.025	0.01	2	0.5

The model uses three separate sets of Van Genuchten parameter to represent the pressure-saturation-hydraulic conductivity relationships; 1) alluvium, 2) weathered bedrock, 3) un-weathered bedrock. The parameters used reflect our understanding that the rock matrix transmits the largest volume of recharge, while recharge through the fractures is faster. The relationships used are biased towards the matrix response. These values were further calibrated using the groundwater level responses and the stream flow. Further rock core samples indicate a high moisture content ($\sim 80\%$) indicating that K is often close to K_s and the hydraulic conductivity-saturation curve reflects this understanding.

Author's changes in manuscript: line 204-215. Text added: The surface and subsurface hydrogeologic units include alluvium, fractured weathered and unweathered bedrock comprised of sandstone, siltstone and shale beds of varying thickness, grain size and cementation (Fig. 2 and Fig. 3). The physical properties of these units, derived from previous on-site investigations (Allegre et al., 2016; Quinn et al., 2015; Quinn et al., 2016) and adjusted by calibration, are summarized in Table 2. In particular, our model uses three separate sets of Van Genuchten parameters to represent the pressure saturation-hydraulic conductivity relationships. The parameters used reflect our understanding that the rock matrix transmits the largest volume of recharge (80%), while recharge through the fractures is minimal (20%) (Manna et al., 2017). Therefore, the relationships used are biased towards the matrix response. These values were further calibrated using the groundwater level responses and the streamflow. Further rock core samples indicate a high moisture content (~80%) (Cherry et al., 2009) indicating that K_u is often close to K_s and the hydraulic conductivity-saturation curve reflects this understanding.

11) Comment from Referee: L 242, MIKESHE, MIKE SHE or MIKE-SHE choose 1 and be consistent.

Author's response: It is MIKE SHE. We made it consistent throughout the text.

12) Comment from Referee: L 265, I would change "centuries" to decades in this sentence.

Author's response: Changed to decades.

13) Comment from Referee: L 270-277 when and how these analysis of samples 24 years old were done? Is it new data, if not, reference? If yes a sentence on the analytical methods.

Author's response: Oxygen isotope ($^{18}\text{O}/^{16}\text{O}$) and hydrogen isotope ($^2\text{H}/^1\text{H}$) ratios were measured on an automated gas-source mass spectrometer at the Center for Isotope Geochemistry at the University of California Berkeley laboratory. Water samples for O-isotope analysis were inlet directly into an automated, computer driven gas equilibration system attached to the mass spectrometer. Hydrogen gas samples were prepared for D/H ratio analysis using conventional reduction methods over heated zinc beads in closed tubes. The hydrogen gas was inlet to the mass spectrometer through an automated inlet system.

Author's changes in manuscript: L329-332. Text added: The available isotope data for rainfall were determined for the period October 1994 to June 1995 collected at two rain gauge stations (B/886 and RMDf), 5 km from the studied watershed and analyzed in the same year by an automated gas-source mass spectrometer at the University of California Berkeley.

14) Comment from Referee: L305-307, I assume these are spatially average recharge rates, if right say it explicitly, if not describe.

Author's response: Correct.

Author's changes in manuscript: This portion of the text was moved to the Model validation (line 456). We added “spatial average” to line 459.

15) Comment from Referee: L 449- 452, typical Mountain Front Recharge (major comment 2).

Author's response: see response to major comment 2

16) Comment from Referee: L 468 see Kurtzman et al., 2016 HESS, for discussion on by-pass preferential flow recharge of fresh water to aquifers under saline unsaturated zone.

Author's response: We added a reference to Kurtzmann et al., 2016 and we also added references regarding the link between precipitation characteristics and preferential flow.

Author's changes in manuscript: Line 550-556: Case studies showing similar results for water that crosses the ET zone preferentially in time and space to become potentially recharge have been also reported in literature (Kurtzman et al., 2016), also referred to as selective recharge (Gat and Tzur, 1967; Florea, 2013; Krabbenhoft et al., 1990) . The occurrence of these fluxes has been also analyzed in function of precipitation characteristics and antecedent water content with rainfall intensity being the main factor (Allocca et al., 2015; Crosbie et al., 2012; Nasta et al., 2018; Taylor et al., 2013).

17) Comment from Referee: Table 3 – rainfall at bottom line is cumulative not mean

Author's response: Correct. We modified accordingly.

18) Comment from Referee: Figure 1. Confusing map. In physical (topographic) maps green is for low lands and brown for high land. Switch the color scale to fit to the customary color scale.

Author's response: We switched the colors according to the reviewer's suggestion.

19) Comment from Referee: Figure 3 enlarge text

Author's response: We increased the size of the text.

20) Comment from Referee: Figure 7 enlarge text. m-1 shouldn't be used for per month (its per meter in the SI system).

Author's response: We changed to “monthly recharge (mm)” to avoid misunderstanding

21) Comment from Referee: Figure all graphics and writing are too small. Panel C is missing.

Author's response: We adjusted all the graphics increasing the font size.

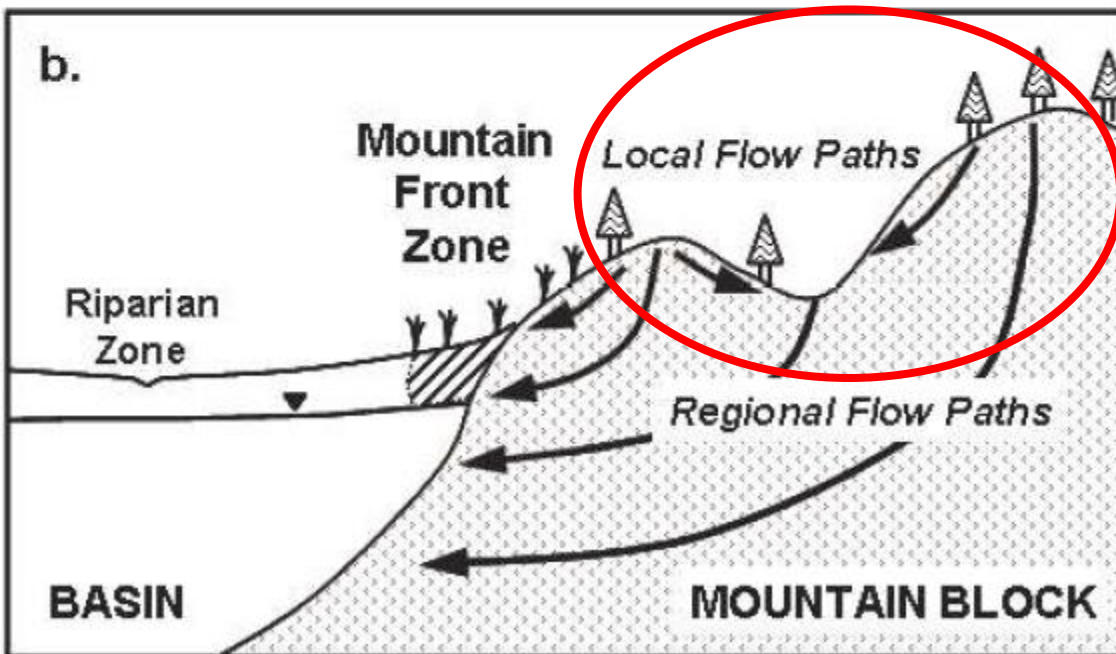
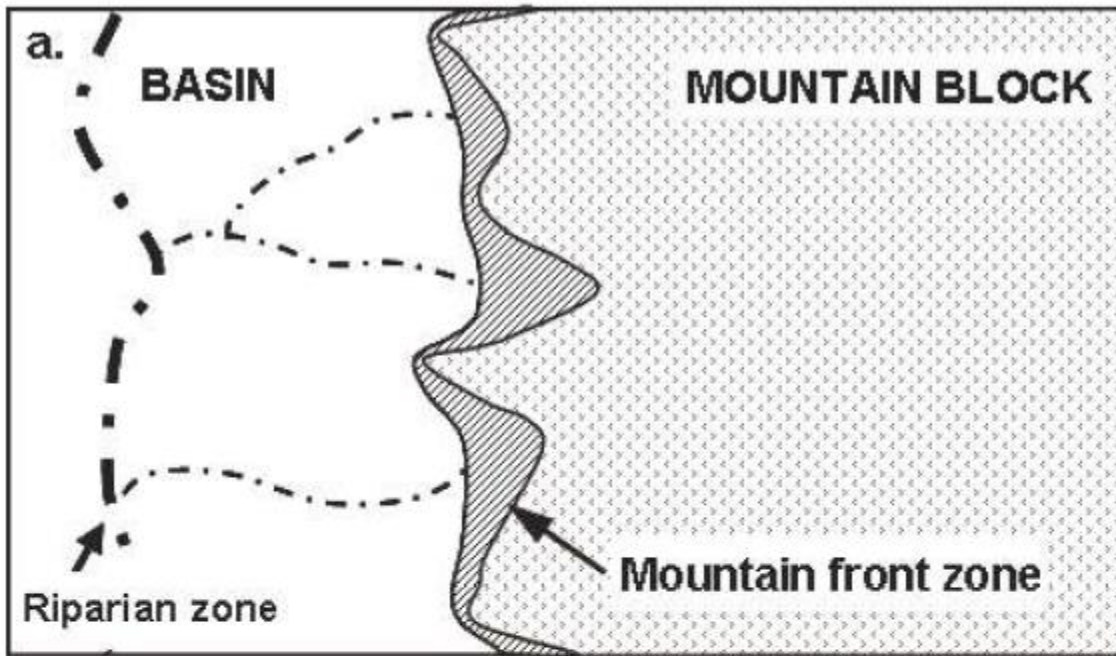


Figure 1. Schematic diagram for Mountain block and Mountain Front Recharge (Figure 2 from Wilson and Guan, 2004). The red circle represents the location of the catchment in this study.

Authors' response to Reviewer 2

General comment

The manuscript describes a modeling study of the spatial and temporal variation of recharge in a 2.16 km² upland catchment in a semi-arid region. Recharge in semi-arid regions constitutes a small fraction of precipitation and is subject to a large temporal and spatial variability. Studies of this hydrological component under semi-arid conditions are relatively few although the references provided by the authors are all more than 10 years old and should thus be updated when revising the manuscript. Nevertheless, I believe that the presented study expands research on recharge in semi-arid regions and that the manuscript deserves publication after revision.

Author's response: We thank Reviewer 2 for the thorough review of the paper and for highlighting the lack of papers using integrated hydrologic numerical models in semi-arid environments. We responded to all the comments and revised the text to improve clarity.

Major comments

1) Comment from Referee: My major concern of the presented work relates to the calibration of the MIKE SHE model, which is inadequately carried out and described. Calibration of a hydrological model should preferably be carried out using an autocalibration method (e.g. PEST) in order to (1) identify the sensitive parameters, (2) calibrate the parameters selected for calibration using an objective method, (3) identify non-uniqueness issues and correlation among the parameters, and (4) identify uncertainty intervals of the calibrated parameter values. The process can be carried out in a more or less sophisticated procedure but in any case it makes the process transparent. The authors do not describe which parameters have been subject to calibration and it is not discussed if the resulting parameters values are reasonable based on prior knowledge of the characteristics of the site. I will encourage the authors to carry out a sensitivity and calibration analysis using an autocalibration method.

Author's response:

The parameters involved in the calibration process were surface roughness, detention storage, imperviousness, rooting depth, Leaf Area Index, crop coefficient, unsaturated hydraulic conductivity and water content parameters of alluvium and weathered bedrock. Although autocalibration would provide more objectivity, we consider our calibration approach to have been rigorous. We tested a wide range of parameter values supported by a large set of field data, against an objective function comprised of groundwater level and stream flow measurements, following a manual trial-and-error history matching approach.

The calibration process proceeded in an iterative manner. After each calibration run, the primary calibration parameters were examined with a variety of metrics including:

Streamflow Calibration Metrics

- Simulated vs Observed Average Annual flow
 - Mean Error
- Simulated vs Observed Average Monthly and Daily Flow:
 - Mean Error
 - Root Mean Squared Error
 - Correlation
 - Nash Sutcliffe Efficiency
- Graphical Plots of Simulated Streamflow Versus Observed Streamflow and Precipitation
 - Provided a qualitative measure of event correlation to observed precipitation and streamflow

Groundwater Level Calibration Metrics

- Simulated versus observed water levels
 - Mean Error
 - Mean Absolute Error
 - Root Mean Squared Error
 - Normalized Root Mean Squared Error
- Graphical Plot of Simulated Vs Observed Water Levels (1:1 residual plot)
 - Provided a quantitative and qualitative assessment of the residual error present at observation wells throughout the domain
- Spatial Plot of Groundwater Residuals (map)
 - Provided a quantitative assessment of water level residuals plotted in the model domain
 - Spatial patterns of fit or misfit of the model were compared against other spatial data (e.g. hydraulic conductivity, boundary conditions, land uses, surface geology) to evaluate potential correlations.

Following an assessment of these calibration targets, model parameters were revised to improve the calibration metrics. During this process our choices were informed by previous knowledge of the site gained over 20 years of investigation. To determine the final value for each of the model parameters, a wide range was explored. For example, for the hydraulic conductivity, the range for the alluvium was from 2×10^{-7} to $5 \times 10^{-4} \text{ m s}^{-1}$ (from 20 to 500% of the final value), whereas for the weathered bedrock the range was from 9×10^{-9} to $3 \times 10^{-5} \text{ m s}^{-1}$ (from 5 to 150% of the final value). For the saturated water content, we explored a range of values for the alluvium from 0.25 to 0.4 and for the weathered bedrock from 0.1 to 0.33.

In instances where the results were not consistent with the site conceptualization, consideration was given as to whether an alternative conceptualization would explain the results predicted by the model. Testing of alternative conceptualizations through manual simulations was chosen over optimization of single conceptualization using software such as PEST given the uncertainty in how to parameterize models in these semi-arid environments. During the calibration, important structural changes were made to the model. For example, to simulate flow in the unsaturated zone, we moved from the simpler gravity flow model to the full Richards equation because the latter better reproduced the natural processes. After few runs, we added an impervious factor to a portion of the bedrock areas where

massive-bedrock ridges were observed. Given these changes and the long processing time of each run (due to the thick vadose zone), it was not possible to carry out an exhaustive optimization or sensitivity analysis. However, through the calibration process we gained semi-quantitative information about the model sensitivity to each parameter.

In particular, we found that the values of unsaturated hydraulic conductivity and water content parameters of alluvium and weathered bedrock had the strongest impact on the calibration targets. These deposits represent the upper layers of our model domain and variations in their physical and hydraulic properties control the rate of infiltration, evapotranspiration, drainage and, therefore, recharge. Another factor with a moderate impact on the generation of streamflow is the detention storage. This is because a significant amount of water from precipitation, especially at the beginning of the rainy season, infiltrates without generating runoff events at the outfall (Fig. 5). This volume of water is controlled not only by the properties of unsaturated zone (Table 2) but also by the value of detention storage assigned to each land use class (Table 1). Conversely, alterations in rooting depth, LAI and crop coefficient only elicited limited changes in streamflow. This is because significant runoff events tend to occur as brief high-intensity precipitation events with a magnitude that far exceeds the relative amount of evapotranspiration which might occur during these events. For the same reason, though, these factors had a relatively greater effect on the volume of water available for drainage and subsequent recharge.

Our confidence about the reasonableness of the final values comes from the fact they are 1) in the same range of those present in literature (Canadell et al., 1996; Scurlock et al., 2001; Chin et al., 2000), 2) similar to those used by the Surface Water Expert Panel to model surface water flow (<https://www.boeing.com/principles/environment/santa-susana/technical-reports.page>), 3) in the range of those measured in the groundwater zone during on-site investigations conducted for 20 years (Cherry et al., 2009). Further confidence regarding the calibrated model and the reasonableness of the final results is derived from the validation process. The latter is based on the comparison with previous independent recharge estimates, evidence from isotopic data sets and analysis of observed fluctuations of water level hydrographs. Moreover, we were satisfied with the fact that all the key processes at the temporal and spatial scale of interest were well represented using the model.

Author's changes in manuscript:

We revised the description of the approach for model calibration (line 254) and model validation (line 300). We also modified the results relative to the calibration (line 343) and validation (line 378)

2) Comment from Referee: My second major concern relates to the conceptualization of the system being studied. The subsurface consists of densely fractured bedrock with parallel beddings and vertical joints and faults leading to preferential flow as also emphasized by the authors at several places in the manuscript. For interpreting chloride and isotope concentration measurements preferential flow appears to be important. Furthermore, the authors have developed a conceptual model for recharge, where distribution between matrix and fractures is described (l. 469-479). The flow processes in and between the two domains are mainly based on speculation and not documented by modelling. The authors need to substantiate why two domains are not considered in their modeling approach.

Author's response: Actually, in a previous published paper, the roles of matrix and preferential flow were examined in detail. Analyzing the different average Cl concentration in the vadose zone and in

groundwater, Manna et al. (2017) estimated that 80% of the recharge occurs as intergranular flow in the porous matrix block and 20% as fracture flow. Therefore, we think that an EPM model, such as MIKE SHE would reproduce accurately the bulk (matrix -predominantly- and fracture) flow in the unsaturated zone. In addition, the spatial resolution (20 by 20 m cells) is such that the dense interconnected network of fractures can be approximated by an EPM model. Our confidence regarding this latter point comes also from the validation of our results, using independently derived data.

The “conceptual model” section includes findings of previous studies that are incorporated and analyzed in the light of the outcome of the present paper to create indeed a conceptual model. This is why we mention the possible occurrence of preferential flow in the deeper vadose zone and describe the potential flow mechanisms, which are not explicitly simulated with MIKE SHE but analyzed in previous studies.

Specific comments

1) Comment from Referee: l. 66-75: Please update literature review with newer references

Author’s response: We updated the literature following also the suggestions of reviewer 1. However, we want to highlight the surprisingly lack of integrated spatially distributed models for semi-arid catchments in recent years.

Author's changes in manuscript: line 64-76. Text added.

Numerical hydrologic models that integrate surface water and groundwater flows have been developed to simulate the spatial and temporal distribution of surface runoff, infiltration, evapotranspiration and groundwater recharge. However, the application of nearly all such simulation tools have been limited to humid regions (Wheater et al., 2007) with minimal application to semiarid regions. Scanlon et al. (2006), in their review on recharge in semiarid areas, reported only 7 papers providing a continuous spatial distribution of recharge, out of a total of 98 studies. However, these studies investigated large areas, from 1,039,647 km² (Flint and Flint, 2007) to 60 km² (Flint et al., 2001), using a relatively coarse spatial resolution (from 72,900 m² - Flint and Flint, 2007 to 900 m² - Flint et al., 2001). In the last decade, although modeling techniques have advanced to include combined surface water-groundwater simulations, recharge in semiarid areas has been represented with a GIS approach (Hernández-Marín et al., 2018) often using remote sensing data (Wang et al., 2008; Coelho et al., 2017; Crosbie et al., 2015) or neglecting the surface water component and focusing on unsaturated zone (Levy et al., 2017; Turkeltaub et al., 2015).

2) Comment from Referee: l. 103-104: As fracture flow is stated to be an important flow process the authors need to substantiate why this flow process is not considered in the modelling.

Author’s response: see response to major comment 2.

3) Comment from Referee: l. 153-156: Is the lateral boundary condition a closed boundary? Is the lower boundary condition based on field measurements? To which extent will it impact the modeling results? Do I understand correctly that groundwater does not contribute to stream flow and that all recharge will to deeper aquifer systems? Please elaborate on the model conceptualization.

Author's response:

There is a fixed head boundary conditions applied to the base and along the lateral faces of the model representing the deep groundwater flow system. The shallow water table and perched systems within the alluvium and weathered bedrock are well above this deeper water table. These heads are based on observed groundwater levels at the site and simulations based on a detailed groundwater flow model. Given that the groundwater heads associated with deep aquifer system are generally observed at relatively large depths below ground surface throughout the domain, it is expected that variations in these specific values assigned would not have a significant effect on predicted recharge values. In areas where the groundwater is observed to be closer to ground surface, the alteration of these values could potentially have a more direct effect on groundwater recharge in that a groundwater table close to the surface could rise to meet the ground surface given sufficient recharge.

It is correct that groundwater contribution to streamflow is intermittent and minimal ($\sim 0.1 \text{ mm y}^{-1}$ for the period of 1995-2014) and only occurs after rainfall event at the farthest downstream location of the catchment where the groundwater table rises close to the ground surface.

Author's changes in manuscript. Line 166 – 174. Text added: A fixed head boundary applied along the lateral sides and the bottom of the model domain (490 m asl) was used to simulate the flow to and from the deeper groundwater system, not explicitly represented in the integrated model but which extends several hundred meters (Fig. 3). These fixed heads are based on observed groundwater levels at the site and simulations based on a detailed 3-D groundwater flow model system that includes the catchment and a much larger domain beyond (AquaResource and MWH, 2007). The groundwater contribution to streamflow is minimal and intermittent ($\sim 0.1 \text{ mm y}^{-1}$ for the period of 1995-2014) and only occurs at the farthest downstream location of the catchment where the groundwater table rises close to the ground surface.

4) Comment from Referee: l. 178-179: What are the thicknesses of the two groundwater zone layers?

Author's response: Layer 1 has a thickness variable from 24 to 185 m (average: 109 m) whereas layer has a uniform thickness of 5 m. While layer 1 may appear very thick the 'active' part from a numerical perspective begin only when the water table is reached. Flow above that occurs in the unsaturated zone that features a finer discretization.

Author's changes in manuscript. Line 196-198 added to the text

5) Comment from Referee: l. 189: Table 2 is incomplete, unsaturated zone characteristics should also be listed.

Author's response: The table has been completed with porosity, field capacity, residual water content and the Van Genuchten parameters (α , n) used in the model.

The model uses three separate sets of Van Genuchten parameter to represent the pressure-saturation-hydraulic conductivity relationships; 1) alluvium, 2) weathered bedrock, 3) un-weathered bedrock. The parameters used reflect our understanding that the rock matrix transmits the largest volume of recharge, while recharge through the fractures is faster. The relationships used are biased towards the matrix response. These values were further calibrated using the groundwater level responses and the stream flow. Further rock core samples indicate a high moisture content (~80%) indicating that K is often close to K_s and the hydraulic conductivity-saturation curve reflects this understanding.

Author's changes in manuscript. New table 2

Hydrogeologic unit	Lithology	K_s ($m\ s^{-1}$)	Saturation (θ_s)	Field capacity (θ_{fc})	Residual Water content (θ_r)	Van Genuchten parameters		
						α	n	l
Alluvium		1×10^{-6}	0.4	0.25	0.05	0.021	1.61	0.5
Weathered bedrock		2×10^{-7}	0.2	0.11	0.01	0.033	1.49	0.5
Unweathered bedrock	Shale/Siltstone	4.1×10^{-10} to 2.3×10^{-7}	0.13	0.1	0.025	0.01	1.23	0.5
Unweathered bedrock	Sandstone	1×10^{-10} to 1×10^{-5}	0.13	0.09	0.01	0.01	2	0.5
Unweathered bedrock	Fault zone	1×10^{-9} to 1×10^{-6}	0.13	0.1	0.025	0.01	2	0.5

6) Comment from Referee: l. 205-211: Could you please be a bit more clear on how the land use are estimated.

Author's response: Land use classes were identified and delineated based on aerial imagery and local land cover datasets (Davis et al., 1998). Descriptions of vegetation classes and species were used in conjunction with literature values for vegetation rooting depth and leaf area indices to describe local vegetation within the model.

7) Comment from Referee: L140 – l. 280- : The calibration procedure needs to be elaborated and revised as described above.

Author's response: see main comment 1.

8) Comment from Referee: l. 301: Generally, I would consider a mean absolute error of 4.5 m to be rather high. Perhaps you mean root mean square error?

Author's response: We agree that 4.5 might be seen as high error. However, we are in a recharge area, on a topographic high with hundreds of meters of head potential. In addition, given the complex structural setting (faults located in the deeper system -not modeled), the heterogeneity of the media (porosity ranging between 2 and 20% within a meter observed in rock cores, hydraulic conductivities between 1×10^{-5} and $1 \times 10^{-10} \text{ m s}^{-1}$), the horizontal and the vertical discretization of the model, we think that 4.5 m is a reasonable mean error.

9) Comment from Referee: l. 303-: To me it would make more sense to compare simulated and observed hydraulic heads directly?

Author's response:

At the transient scale, we do not expect a good matching between simulated and observed head data. This is because of the strong subsurface heterogeneity (see response to comment 8) and because the focused recharge is soon "dissipated" through the fracture system, with head measurements in open borehole blending the contributions of several hydraulically active fractures. However, these flow dynamics in the groundwater zone are beyond the scope of this paper. This is why to validate the ability of the model to reproduce transient conditions, we compared the spatially-average simulated recharge against the observed heads, representing the bulk response of the system to the recharge input.

10) Comment from Referee: l. 316- 318: Perhaps the equivalent porous medium approach is suitable for simulation of water flow but for solute transport and the interpretation of chloride and isotopes I am not sure.

Author's response: Agree but this is truer for the saturated zone than for the vadose zone. As explained in the response to the main comment 2, a previous study found that at the site recharge occurs mainly as intergranular matrix flow in the vadose zone. Therefore, we think that our EPM model can be corroborated by recharge studies based on the Chloride Mass Balance method and that the isotopic composition of groundwater can be interpreted under an EPM conceptual model (especially because the ET zone is made of alluvium and weathered bedrock).

11) Comment from Referee: l. 352: Fig. 8a and 8b.

Author's response: Ops! We replaced 7b with 8b.

12) Comment from Referee: l. 373: Check consistency with lines 216-217.

Author's response: Thanks. We made it consistent.

1 **Spatial and temporal variability of groundwater recharge in a sandstone**
2 **aquifer in a semi-arid region**

3 **Ferdinando Manna** ¹, **Steven Murray** ², **Daron Abbey** ², **Paul Martin** ^{2,3}, **John Cherry** ¹,
4 **Beth Parker** ¹

5 ¹ G³⁶⁰ Institute for Groundwater Research, College of Engineering and Physical Sciences,
6 University of Guelph, Guelph, Ontario, Canada ~~University of Guelph, Ontario, Canada~~

7 ² Matrix Solutions Inc., Guelph, Ontario, Canada

8 ³ Aqua Insight Inc., Waterloo, Ontario, Canada.

9

10 **Abstract**

11 With the aim to understand the spatial and temporal variability of groundwater recharge, a high-
12 resolution, spatially-distributed numerical model (MIKE SHE) representing surface water and
13 groundwater was used to simulate responses to precipitation in a 2.16 km² upland catchment on
14 fractured sandstone near Los Angeles, California. Exceptionally high temporal and spatial resolution
15 was used for this catchment modeling: ~~an hourly~~ time-step climate data, a 20x20 meter grid in the
16 horizontal plane and 240 numerical layers distributed vertically within the thick vadose zone and in
17 the upper part of the groundwater zone. The finest-practical spatial and temporal resolution were
18 selected to accommodate the large degree of surface and subsurface variability of catchment features.
19 Physical property values for the different lithologies were assigned based on previous on-site
20 investigations whereas the parameters controlling streamflow and evapotranspiration were derived
21 from ~~calibration to literature information.~~ The calibration of continuous streamflow at the outfall
22 and ~~to of transient and~~ average hydraulic heads from 17 wells. ~~provided confidence in the~~
23 ~~reasonableness of these input values and in the ability of the model to reproduce observed processes.~~
24 Confidence in the calibrated model was enhanced by validation through, i) comparison of simulated

25 average recharge to estimates based on the applications of the chloride mass-balance method ~~from~~
26 ~~to~~ data from the groundwater and vadose zones within and beyond the catchment (~~Manna et al.,~~
27 ~~2016; Manna et al., 2017~~) and, ii) comparison of the water isotope signature (^{18}O and ^2H) in shallow
28 groundwater to the variability of isotope signatures for precipitation events over an annual cycle ~~and,~~
29 iii) comparison of simulated recharge time series and observed fluctuation of water levels. The
30 average simulated recharge across the catchment for the period 1995-2014 is 16 mm y^{-1} (4% of the
31 average annual precipitation), which is consistent with previous estimates obtained by using the
32 chloride mass balance method (4.2% of the average precipitation). However, one of the most
33 unexpected results was that local recharge was simulated to vary from 0 to $> 1000 \text{ mm y}^{-1}$ due to
34 episodic precipitation and overland runoff effects. This recharge occurs episodically with the major
35 flux events at the bottom of the evapotranspiration zone, as simulated by MIKE SHE and confirmed
36 by the isotope signatures, occurring only at the end of the rainy season. This is the first study that
37 combines MIKE SHE simulations with the analysis of water isotopes in groundwater and rainfall to
38 determine the timing of recharge ~~processes~~ in a sedimentary bedrock aquifer in a semi-arid regions.
39 The study advances the understanding of recharge and unsaturated flow processes ~~in semi-arid~~
40 ~~regions~~ and enhances our ability to predict the effects of surface and subsurface features on recharge
41 rates. This is crucial in highly heterogeneous contaminated sites because different contaminant
42 source areas have widely varying recharge and, hence, groundwater fluxes impacting their mobility.

43 **Introduction**

44 Assessment of groundwater recharge is fundamental to create strategies for management of water
45 resources and to estimate volumetric groundwater flow through contaminated sites. Recharge rates
46 represent an indication of upper limit of the volume of precipitation that may be accessible for
47 sustainable use and can govern the volume of water available to transport contaminants. Its
48 importance is greater in semi-arid regions where dominance of evapotranspiration limits water

49 resources. In these regions, estimated recharge rates depend on the temporal and spatial resolution
50 of the investigation and the uncertainties associated with recharge values are usually large
51 (Scanlon, 2000; Xie et al., 2018; Crosbie et al., 2018). In favorable circumstances, geochemical-based
52 methods have proven to be especially useful for estimating recharge rates. In areas where the
53 geologic and anthropogenic sources of chloride in the subsurface are negligible, ~~the natural the~~
54 ~~distribution of~~ chloride in the vadose zone and groundwater, ~~deriving from atmospheric~~
55 ~~deposition~~, has been used to calculate long-term site-wide (Wood and Sanford, 1995; Gebru and
56 Tesfahunegn, 2018; Jebreen et al., 2018) and location-specific recharge values (Heilweil et al., 2006;
57 Huang et al., 2018), ~~to~~ determine mechanisms of flow in the vadose zone (Sukhija et al., 2003; Li et
58 al., 2017), ~~and to~~ evaluate the effects of environmental changes on recharge ~~process~~ (Scanlon et al.,
59 2007; Cartwright et al., 2007). Elevated tritium in precipitation derived from atmospheric releases
60 during nuclear tests in the 1960's and transported into the subsurface has also been an invaluable
61 tracer to determine modern recharge and mechanisms of flow in both vadose and groundwater
62 zones (Cook and Böhlke, 2000; De Vries and Simmers, 2002). These geochemical and isotopic
63 techniques are based on the interpretation of hydrologic process influences on the distribution of
64 tracers in the subsurface but cannot show the ~~transient-dynamic, short-term temporal~~ effects nor
65 provide a continuous spatial representation of these processes at the catchment scale.

66 Numerical hydrologic models that integrate surface water and groundwater flows have been
67 developed to simulate the spatial and temporal distribution of surface runoff, infiltration,
68 evapotranspiration and groundwater recharge. However, the application of nearly all such
69 simulation tools have been limited to humid regions (Wheater et al., 2007) with minimal
70 application to semiarid regions. Scanlon et al. (2006), in their review on recharge in semiarid areas,
71 reported only 7 papers providing a continuous spatial distribution of recharge, out of a total of 98
72 studies. ~~However, these studies were conducted at Yucca Mountain, Hanford site, Death Valley~~
73 ~~region, Great Basin, the semiarid southwestern US and in the State of Nebraska and~~ investigated

74 large areas, from 1,039,647 km² (Flint and Flint, 2007) to 60 km² (Flint et al., 2001), using a
75 relatively coarse spatial resolution (from 72,900 m² - Flint and Flint, 2007 to 900 m² - Flint et al.,
76 2001). In the last decade, [although modeling techniques have advanced to include combined](#)
77 [surface water-groundwater simulations, modeling techniques have advanced to include combined](#)
78 [surface water-groundwater simulations, recharge in semiarid areas has been represented with a](#)
79 [GIS approach](#) (Hernández-Marín et al., 2018) [often using remote sensing data](#) (Wang et al., 2008;
80 Coelho et al., 2017; Crosbie et al., 2015) [- or neglecting the surface water component and focusing](#)
81 [on unsaturated zone](#) (Levy et al., 2017; Turkeltaub et al., 2015).

82 Among the commercially available models, the physically based MIKE-SHE represents the land-
83 based hydrologic system, with an integration of the surface flows (i.e. precipitation, infiltration,
84 evapotranspiration and runoff) and subsurface flows (i.e., percolation into the vadose zone and
85 recharge across the water table) (Ma et al., 2016). However, the literature shows only two
86 applications of MIKE SHE to assess recharge in semiarid areas. Liu et al. (2007) analyzed the
87 recharge response associated with overland flow in an alluvial watershed (surface area: 91 km² -
88 cell size: 2,500 m²) in the Tarim Basin, China. Smerdon et al. (2009) distinguished and quantified
89 the contributions of three sources to the total recharge for a valley bottom aquifer in the
90 ~~Okanagan~~Oakanagan Basin (Canada) (surface area: 130 km² - cell size: 10,000 m²).

91 In this study encompassing a 20-year period (1995-2014), we used MIKE SHE to simulate the
92 recharge and the other hydrologic processes in a small catchment (2.16 ~~km²~~km²) located on an
93 exposed bedrock upland plateau (from 650 to 490 m asl) in the Simi Hills, near Los Angeles,
94 California (Fig. 1). The area is semi-arid with potential evapotranspiration (CIMIS, 1999) exceeding
95 the average annual precipitation (396 mm as the recorded average annual precipitation over the
96 1995 -2014 period). The bedrock consists of sandstone with interbeds of shale and siltstone,
97 densely fractured with bedding parallel partings and vertical joints and faults (Cilona et al., 2015;
98 Cilona et al., 2016; Link et al., 1984; MWH, 2016) (Fig. 2). The hydrogeology of the site has been

99 investigated intensively over the past 20 years because of the chemical contamination ([mainly](#)
100 [Trichloroethene - TCE](#)) in groundwater (Pierce et al., 2018a; Pierce et al., 2018b; Sterling et al.,
101 2005; MWH, 2009; Cherry J.A., 2009) and construction [and application](#) of a 3-D flow model
102 (FeFlow) has been an on-going effort [supporting characterization and corrective measures](#)
103 (AquaResource and MWH, 2007). ~~For this model, information about the spatial distribution of~~
104 ~~recharge is needed as an upper boundary condition and to refine results of previous studies.~~ From
105 the application at the site of the chloride mass balance (CMB), based on measurement of chloride in
106 atmospheric deposition, surface water and groundwater, Manna et al. (2016) estimated a long-term
107 average recharge of 19 mm y⁻¹, corresponding to the 4.2 % of the average precipitation (455 mm for
108 the period 1878-2014). More recently, Manna et al. (2017) analyzed porewater Cl concentration
109 profiles from the vadose and groundwater zones at 11 locations across the site. This provided
110 spatially variable, long-term recharge values ranging from 4 to 23 mm y⁻¹ and indicated that, on
111 average, 80% of the flow in the vadose zone occurs as intergranular flow in the rock matrix and
112 20% as fracture flow. ~~However, T~~these chloride-based methods lump together hydrologic
113 processes providing long-term recharge estimates for only few locations across a large site.

114 ~~However, to inform the 3-D groundwater flow model and to simulate plume fluxes, For this model,~~
115 ~~information about the spatial and temporal distribution of recharge is needed as an upper~~
116 ~~boundary condition and to refine results of previous studies.~~

117 In this study, we analyze the spatial and temporal variability of recharge in a catchment [of the](#)
118 [contaminated site not only to constrain recharge values but also to uncover hydrologic processes](#)
119 [that cause the borehole-scale spatial variability observed in those previous studies](#) (Manna et al.,
120 2016; Manna et al., 2017). ~~representative of the varied surface and subsurface conditions found~~
121 ~~throughout the contaminated area.~~ The catchment was chosen [because it is representative of the](#)
122 [varied surface and subsurface conditions found throughout the contaminated area and also because](#)
123 it is believed to be [minorly minimally](#) impacted during the calibration period by the surface water

124 controls measures in place. Given that the scope of the paper is to simulate the natural conditions,
125 these initiatives are not considered in our modeling. ~~To~~To better represent the large range of
126 surface and subsurface features and provide high-resolution representation of the spatial
127 distribution of recharge, we used ~~an hourly climate data, sub-hourly time step hourly time step~~ and
128 a fine grid of 400 m² cells for a total of 5,420 cells. In addition to the spatial variability, we also
129 examined the seasonal dynamics of the hydrologic processes by tracking vadose zone water
130 budgets for representative cells of the model. This analysis helped in understanding the transient
131 conditions that determine the rates of the hydrologic processes throughout the year. The model
132 was calibrated using measurements of runoff from instrumented outfall flows and quarterly
133 observations of groundwater levels in 17 wells distributed across the catchment for the simulated
134 period. Unlike the previous applications of MIKE SHE in the literature, ~~T~~he simulation results were
135 also validated through comparison with transient water levels from shallow wells, comparison with
136 previous independent recharge estimates based on application of the Chloride Mass Balance
137 (Manna et al., 2016; Manna et al., 2017) and through the analysis of water isotopes from rainfall and
138 groundwater that indicated the timing of recharge. Finally, we proposed a conceptual model for
139 various recharge conditions in the fractured sandstone aquifer based on the results of the MIKE
140 SHE simulation along with findings of previous recharge studies for the site (Manna et al., 2016;
141 Manna et al., 2017). In particular, the MIKE SHE simulations contributed to the conceptual model
142 concerning the role of surface feature variability-(e.g. topography and vegetation) on the
143 hydrological processes whereas the Cl-based studies informed the flow mechanisms in the
144 underlying portion of the system.

145

146 **The site MIKE SHE model**

147 The MIKE SHE model (Refsgaard, 1995) simulations were ~~completed~~ conducted at ~~an a~~ sub-hourly
148 time step using ~~the~~ hourly meteorological data measured from 1995 through 2014 on site and from
149 stations proximal to the study area ~~from 1995 through 2014~~. A portion of the rainfall is intercepted
150 by the vegetation canopy, from which evaporation occurs. The remaining water reaches the surface,
151 where it may infiltrate, evaporate or runoff downslope if depression storage is satisfied. Water
152 infiltrating into the subsurface may be evapotranspired back to the atmosphere or percolate down
153 to the water table to become groundwater recharge. infiltrating into the subsurface with some
154 ~~transpired back to the atmosphere.~~ Actual evaporation and transpiration were simulated based on
155 the Kristensen and Jensen Evapotranspiration Model (Kristensen and Jensen, 1975), which
156 considers potential evapotranspiration estimated using the FAO 56 Penman-Monteith method
157 (Allen et al., 1998), available soil moisture and the crop characteristics (depth of the
158 evapotranspiration zone, leaf area index and crop coefficient) in each grid cell (Table 1). When the
159 rainfall exceeds the infiltration capacity, water is ponded on the ground surface and is available for
160 runoff. The infiltration capacity in the model is dynamic and a function of the unsaturated hydraulic
161 conductivity (K_u) and the water content properties (i.e., saturation point, field capacity and
162 permanent wilting point) of the surficial media. To describe the relation between water content,
163 conductivity and matric potential, the Van Genuchten model is used (Van Genuchten, 1980). The
164 rate of runoff is simulated using a 2D diffusive wave approximation and is controlled by the
165 topographic slope, the surface roughness and detention storage. The latter is the volume of water
166 stored in surface depressions before runoff starts. The unsaturated zone flow is simulated as the
167 change in soil moisture, ~~as a r~~ resulting from ~~of~~ cyclical input (infiltration) and output (recharge and
168 evapotranspiration). It is modelled as a 1D column using the full Richards equations (Richards,
169 1931) with finite difference cells that have variable discretization from the top of the column
170 (ground surface) to the base of the column (the unsaturated/saturated zone interface). ~~It is mainly~~
171 ~~vertical, because gravity is the foremost forcing factor and is simulated using the full Richards~~

172 ~~equation~~. Given the variable thickness of the vadose zone and the low water fluxes, the model was
173 run several times to set ~~proper~~ consistent initial conditions. Our analysis began when the
174 simulation showed that the degree of change in average recharge value from one run to the next
175 was about 0.3% indicating near steady-state conditions. Recharge was calculated anytime that
176 infiltration water arrives at the water table, ~~recognizing that m~~ Most precipitation events do not
177 result in recharge because infiltration into the shallow subsurface ~~which~~ is intercepted and
178 evapotranspired ~~before it can become groundwater recharge~~. The ~~saturated zone~~ flow in the
179 groundwater zone was represented using 3D finite difference Darcy equation. A fixed head
180 boundary applied along the lateral sides and from the bottom of the model domain (490 m asl) was
181 used to simulate the flow to and from the deeper groundwater system, not explicitly represented in
182 the integrated model but which extends several hundred meters ~~and thus was not explicitly~~
183 ~~represented in the integrated model~~ (Fig. 3). These fixed heads are based on observed
184 groundwater levels at the site and simulations based on a detailed 3-D groundwater flow model
185 system that includes the catchment and a much larger domain beyond (AquaResource and MWH,
186 2007). The groundwater contribution to streamflow is minimal and intermittent (~ 0.1 mm y⁻¹ for
187 the period of 1995-2014) and only occurs at the farthest downstream location of the catchment
188 where the groundwater table rises close to the ground surface.

189 *Climate data*

190 Hourly rainfall data were collected from two stations within the catchment boundaries: the Sage
191 Ranch station, managed by Ventura County watershed
192 (<http://www.vcwatershed.net/hydrodata/php/getstation.php?siteid=272#top>) and the Simi Hills-
193 Rocketdyne Lab, managed by Boeing Inc. The annual precipitation ranges from 99 mm (2014) to
194 976 (1998), with an average value of 396 mm y⁻¹. The seasonal precipitation regime is
195 Mediterranean, with 77% of the total precipitation occurring from December to March.

196 Daily maximum and minimum air temperature observations were obtained from two climate
197 stations of the NOAA network: from 1995 to 1998 data were gathered from the Cheeseboro station
198 (<https://www.ncdc.noaa.gov/cdo-web/datasets/GHCND/stations/GHCND:USR0000CCHB/detail>)
199 and from 1998 to 2015 from the Van Nuys station (<https://www.ncdc.noaa.gov/cdo->
200 [web/datasets/GSOM/stations/GHCND:USW00023130/detail](https://www.ncdc.noaa.gov/cdo-web/datasets/GSOM/stations/GHCND:USW00023130/detail)), respectively 6 km SW and 18 km E
201 of the study site. Temperatures were adjusted using a dry ($10\text{ }^{\circ}\text{C km}^{-1}$) and wet ($5.5\text{ }^{\circ}\text{C km}^{-1}$)
202 adiabatic lapse rate based on the elevation change between the SSFL site and the collecting station.
203 July, August and September are the warmest months with an average daily maximum temperature
204 of 30.5, 31 and 30.4 $^{\circ}\text{C}$, respectively whereas February and December are the coldest with an
205 average daily maximum temperature of 17 and 17.4 $^{\circ}\text{C}$, respectively. Annual average temperature is
206 16.7 $^{\circ}\text{C}$.

207 *Surface and subsurface parameters*

208 The MIKE SHE model was developed employing a 20 by 20 m ~~finite-finite~~-difference ~~horizontal~~
209 ~~horizontal~~-plane grid to represent the surface ~~variation in~~-physical features, a fine vertical
210 discretization of the vadose zone with 240 numerical layers ranging from 0.1 to 1 m thickness and 2
211 groundwater zone layers, with thickness variable from 5 to 185 m, to represent vertical variability
212 at, and just below, the position of the water table (Fig. 3). This resolution was selected as a
213 compromise between representation of spatial variability at a more detailed scale and reasonable
214 computational time. Maps of topography, vegetation, surficial geology and land use were used to
215 assign surface parameters (Fig. 1, Fig. 2 and Fig. 4). High resolution topographic data (2 feet
216 interval elevation contours) were obtained based on an aerial survey of the site in 2010. These
217 topography data were used to define the ground surface elevations (Fig. 1). ~~High resolution~~
218 ~~topographic data (2 feet interval elevation contours) were obtained based on an aerial survey of the~~
219 ~~site in 2010. These topography data were used to define the ground surface elevations (Fig. 1).~~

220 The surface and subsurface hydrogeologic units include alluvium, fractured weathered and
221 unweathered bedrock comprised of sandstone, siltstone and shale beds of varying thickness, grain
222 size and cementation (Fig. 2 and Fig. 3). The physical properties of these units, derived from
223 previous on-site investigations (Allegre et al., 2016; Quinn et al., 2015; Quinn et al., 2016) and
224 adjusted by calibration, are summarized in Table 2. In particular, our model uses three separate
225 sets of Van Genuchten parameters to represent the pressure saturation-hydraulic conductivity
226 relationships. The parameters used reflect our understanding that the rock matrix transmits the
227 largest volume of recharge (80%), while recharge through the fractures is minimal (20%) (Manna
228 et al., 2017). Therefore, the relationships used are biased towards the matrix response. These
229 values were further calibrated using the groundwater level responses and the streamflow. Further
230 rock core samples indicate a high moisture content (~80%) (Cherry et al., 2009) indicating that K_u
231 is often close to K_s and the hydraulic conductivity-saturation curve reflects this understanding.

232 Four land use classes were identified and delineated based on aerial imagery and local land cover
233 datasets (Davis et al., 1998): developed areas (roads, building, parking lots); chaparral (chamise,
234 scrub oak), coastal scrub (Black sage) and exposed bedrock (areas without vegetation) (Fig. 4). The
235 first category represents only 5% of the study catchment whereas the two vegetation classes
236 (chaparral and coastal sage scrub) cover 83% of the area. The remaining 12% is represented by
237 areas of bedrock outcrop at surface. This latter category was subdivided into two classes: non-
238 massive bedrock and massive bedrock based on physical appearance. Massive bedrock areas were
239 identified based on rock masses that have resisted erosion over the decades and are presumed to
240 be poorly-fractured and/or well cemented such that local infiltration through these rock units is
241 very low. These cells-cell assignments were identified using topography and imagery analysis. First,
242 we used the minimum downslope elevation change approach to identify topographic ridges; this
243 algorithm calculates the minimum elevation drop to a downslope neighbor. In a second stage, we
244 isolate from the land use map the exposed bedrock areas. Vegetation, indeed, indeed, is unlikely to

245 generally does not grow on well cemented rock. Finally, massive bedrock areas were identified
246 assigned as cells with downslope elevation change greater than 1.25 meters in areas without
247 vegetation.

248 Values of Leaf Area Index, depth of the root zone, surface roughness and Manning's number were
249 assigned to each land use class-specific parameters, were assigned based on the calibration
250 process, with final values similar to those available in the literature values (Canadell et al., 1996;
251 Scurlock et al., 2001; Chin et al., 2000) (Table 1). To calculate the actual evapotranspiration, Aa
252 crop coefficient varying monthly between 0.53 and 1.02 has been calculated used for the site. The
253 This estimates are based on i) reference crop evapotranspiration rates (RET) for Zone 9 of the
254 Reference Evapotranspiration Zones map of the California Irrigation Management Information
255 System, that corresponds with the area the site is within (ITRC, 2003), ii) a 'Pasture and Misc.
256 grasses' land class chosen as representative of the site and iii) a reduction of 8% to account for bare
257 spots in vegetation and reduced vigor (ITRC, 2003).

258 *Unsaturated zone water budgets*

259 To assess the temporal variability of infiltration, evapotranspiration, change in storage and
260 recharge recharge and other hydrologic processes, we extracte analyzed the simulated unsaturated
261 zone water budgets for two locations representing the span of variability of the catchment. The two
262 locations were selected based on surface geology (Fig. 2) and land use category (Fig. 4): UZ1
263 represents an area of outcropping bedrock without vegetation a cell with alluvium at the surface
264 covered by vegetation, whereas and UZ2 represents a cell with alluvium at the surface and
265 vegetation covered by vegetation an area of outcropping bedrock without vegetation. The average
266 infiltration value over the simulated period at the two locations (UZ-1: 87 mm y⁻¹; UZ-2: 395 mm y⁻¹)
267 matches the average infiltration value for all the cells of the catchments with same land use and
268 surface geology geology characteristics. For these cells, we extracted the weekly time series of

269 infiltration, evapotranspiration, storage variations and flux at the bottom of the ET zone (i.e.,
270 drainage). The latter indicates the volume of water that infiltrates into the vadose zone and will
271 eventually become recharge upon reaching the water table. The analysis of the seasonal variability
272 of these fluxes provided insights about their transient nature and about the effect of the surface
273 variability on the hydrologic processes in the unsaturated zone.

274 *Approach for model calibration ~~and validation~~*

275 In the model calibration procedure, the simulation results were compared to observed processes
276 and, to obtain acceptable matches, 10 parameters were available to adjust: In this study, calibration
277 refers to a test of the ability of the model to reproduce observed processes and to evaluate values of
278 model parameters, for which measurements are not available. On the other hand, validation is the
279 comparison of model results with alternative data, independently derived, to provide confidence
280 about the reasonableness of the results.— surface roughness, detention storage, imperviousness,
281 rooting depth, leaf area index (LAI), crop coefficient, unsaturated hydraulic conductivity and water
282 content parameters of alluvium and weathered bedrock. These were tested against an objective
283 function of streamflow and groundwater level measurements. An objective function is a measure of
284 overall model fit of simulated to observed values of groundwater levels and streamflow.

285

286 ~~To calibrate the integrated surface water and groundwater model, we compared i) the simulated~~
287 ~~and observed runoff flow at the outfall of the catchment, ii) the simulated and observed average~~
288 ~~groundwater head data from 17 wells located within the catchment area and iii) the simulated time~~
289 ~~series of recharge and the observed fluctuations of water level hydrographs. For the purpose of~~
290 streamflow calibration, we compared the surface runoff generated by MIKE SHE to the data
291 collected at the catchment outfall between 2009 to 2011. This time interval had minimal

292 occurrence of substantial anthropogenic activities and was representative of natural hydrologic
293 conditions, as reported also by Manna et al. (2016).

294 For the calibration ~~of to~~ groundwater levels, quarterly manually measured water level data
295 ~~measured manually~~ were used. Excluded from the calibration data were: i) wells with screened
296 interval below the bottom of the model domain (490 m a.s.l.), and ii) wells where the water table is
297 strongly influenced by subsurface complexity not represented in the saturated zone portion of the
298 MIKE_SHE model. ~~This resulted in~~ After these exclusions, water level data from 17 wells being used
299 with water depths ranging from 25 to 137 meters bgs (Fig. 1, 2 and 4). The number of
300 measurements in the time series at each well varies from 1 (RD-130) to 139 (WS-09B)
301 measurements. In the calibration procedure, a Average values were used for comparison with
302 average simulated values ~~to judge the spatial distribution of model parameters.~~

303 The calibration process proceeded in an iterative manner. After each calibration run, the two
304 calibration targets were examined with a variety of metrics. For the streamflow, we analyzed mean
305 error for simulated and observed average annual flow; mean error, root mean squared error,
306 correlation and Nash Sutcliffe Efficiency for the simulated and observed average monthly and daily
307 flows. An additional qualitative measure of the correlation between precipitation and streamflow
308 event was provided by the analysis of the graphical of plots of observed and simulated daily
309 streamflow hydrographs.

310 For the groundwater levels, the metrics were mean error, mean absolute error, root mean squared
311 error and normalized root mean squared error for the simulated and observed average water
312 levels. In addition, residual plots of simulated and observed water levels provided a quantitative
313 and qualitative assessment of the residual error present at the observation well throughout the
314 domain. Spatial patterns of groundwater level residual were compared against other spatial data

315 (e.g. hydraulic conductivity, boundary conditions, land uses, surface geology) to evaluate potential
316 correlations and adjustments that could improve the calibration.

317 Following an assessment of these calibration targets, the ten model parameters were adjusted for
318 better calibration metrics. In instances where the results were not consistent with the site
319 conceptualization, consideration was given as to whether an alternative conceptualization would
320 explain the results predicted by the model. Testing of alternative conceptualizations through
321 manual simulations was chosen over the alternative method of optimization of a single
322 conceptualization using software such as PEST (Doherty, 2004) given the uncertainty in how to
323 parameterize models in these semi-arid environments. Given the structural changes
324 (representation of the unsaturated flow, representation of impervious areas) that were made to the
325 model during the several simulations, it was not possible to carry out an exhaustive optimization or
326 sensitivity analysis. However, through the calibration process we gained semi-quantitative
327 information about the model sensitivity to each parameter which is presented in the results section.

328

329 *Approach for model validation*

330 To obtain confidence about the reasonableness of the results, simulation results from the
331 calibrated model were tested by a validation procedure, which included comparison ~~Furthermore,~~
332 ~~to test the ability of the model to simulate unsaturated zone flow processes and to reproduce the~~
333 ~~transient recharge conditions, we compared the simulated time series of recharge, obtained from~~
334 ~~MIKE SHE, with quarterly water level measurements at five locations. The depth to groundwater at~~
335 ~~these wells ranges between 2 and 60 m with seasonal fluctuations due to the recharge events. The~~
336 ~~recharge time series is obtained, extracting the average, catchment wide, monthly recharge values.~~

337 ~~Simulation results were validated based on the comparison with~~to previous independent recharge
338 estimates based on chloride and, and timing of recharge from evidence from isotopic data sets(¹⁸O

339 - ^{2}H) and from analysis of observed fluctuations of water level hydrographs, not used in the
340 calibration. The premise of the validation is that the calibrated model must provide results
341 consistent with the validation information, that are entirely independent of the parameter
342 assignments made in the calibration.

343 Manna et al. (2016) estimated an average long-term recharge of 19 mm y⁻¹ for the same catchment
344 using the chloride mass balance (CMB) method, based on the average Cl concentration measured in
345 the atmospheric deposition, comprised of rainfall and dry fallout (2.6 mg L⁻¹), surface water at the
346 catchment outfall (4 mg L⁻¹) and groundwater (52.5 mg L⁻¹). Since chloride concentration in
347 groundwater is proportional to the concentrating effect of water loss due to evapotranspiration, it
348 can be used as a proxy to determine the range of variability in recharge. Chloride concentration in
349 shallow groundwater monitoring wells ranges across the area from 17 to 162 mg/L corresponding
350 to recharge values of 43 and 5 mm y⁻¹, respectively. Manna et al (2017) also provided insights
351 regarding spatial variability of recharge within the catchment based on analysis of Cl profiles in
352 porewater from the vadose zone and groundwater ~~and which~~ indicated a range of recharge from 4
353 to 21 mm y⁻¹ corresponding to <1 – 4.7% of the average annual precipitation for 4 locations located
354 within the catchment area. Although the recharge values obtained from the CMB method integrate
355 hydrologic processes occurring over longer time, from ~~centuries-decades~~ to millennia, they
356 represent a reasonable assessment of long-term, site-wide and location-specific average values and
357 are valuable for validation purposes.

358 ~~For the validation of the unsaturated zone water budget, s~~ Samples of rainfall and groundwater
359 were analyzed for water isotopes (^{18}O – ^{2}H) (~~oxygen-18 and deuterium~~). ~~These W~~ water isotopes
360 are commonly used to assess evaporative processes and to determine sources and origins of
361 different groundwaters. Typically, the water isotope values vary seasonally over the annual cycle,
362 so that the groundwater composition reflects the season with most of the recharge. In this study,
363 we compared the isotopic signature of groundwater to that of precipitation for an entire

386 hydrological year to determine whether the timing of recharge indicated by the model is consistent
387 with the isotopic signature for the same period of the year. The available isotope data for rainfall
388 ~~For this purpose we used 1) were determined for the period rainfall samples collected from~~
389 October 1994 to June 1995 collected at two rain gauge stations (B/886 and RMDF) ~~located in a~~
390 ~~different portion of the site~~, 5 km from the studied watershed and analyzed in the same year by an
391 automated gas-source mass spectrometer at the University of California Berkeley. The -and 2)
392 groundwater samples were collected from monitoring wells in the studied catchment in two rounds
393 of sampling: the first in 2003-2004 and the second in 2013 (Fig. 1).

394 Furthermore, to test the ability of the model to simulate unsaturated zone flow processes and to
395 reproduce the transient recharge conditions, we compared the simulated time series of recharge,
396 obtained from MIKE SHE, with quarterly water level measurements at five locations not used in the
397 calibration process. The depth to groundwater at these wells ranges between 2 and 60 m with
398 seasonal fluctuations due to the recharge events. The recharge time series is obtained, extracting
399 the average, catchment-wide, monthly recharge values.

400

401 **Simulation Results and discussion**

402 *Model calibration and sensitivity*

403 ~~The ability of the model to reproduce observed conditions has been investigated to provide~~
404 ~~confidence that the model can be used to simulate the spatial and temporal variation in recharge~~
405 ~~and other water budget components. This ability to represent measured surface and sub-surface~~
406 ~~flows depends on the reasonableness of the input parameters assigned to the different land use and~~
407 ~~lithology classes (Table 1 and 2).~~

Format

408 ~~When analyzing measured data, s~~Streamflow measured at the outfall ~~is observed~~occurs -in
409 response to rainfall; ~~but interestingly~~however, some precipitation events are followed by very low
410 or no measurable flow (Fig. 5). This is evident for precipitation events from April to June 2009,
411 October and November 2010 and May and June 2011. In all these cases, the surface runoff,
412 generated by the precipitation events, infiltrates into the subsurface without reaching the surface
413 outfall (Fig. 5). These hydrologic dynamics are well simulated by MIKE SHE. The comparison
414 between the observed and the simulated hydrographs shows a good correlation for the calibration
415 period ($R^2=0.97$; average difference 4.7%). The average simulated flow is 48 mm y^{-1} , about 14.5% of
416 the average precipitation for the 2009-2011 period (331 mm) and is almost coincident with the
417 measured flow (46.2 mm y^{-1}) (Fig. 5). This value reflects the precipitation conditions of the 2009-
418 2011 period and is lower than the average runoff over the entire simulated interval (110 mm y^{-1} ,
419 28% of the annual precipitation). Monthly and daily Nash Sutcliffe Efficiency (NSE) values of 0.94
420 and 0.87 were achieved respectively, indicating good fit to observed flows (NSE=1 corresponds to a
421 perfect match).

422 In addition to the surface water leaving the catchment, the model was also calibrated ~~by comparing~~
423 ~~simulated and to the~~ observed average groundwater head data (Fig. 6). ~~The two sets of data show~~
424 ~~a~~ good match was obtained for the 17 locations, with almost all values falling within the 10 m
425 confidence interval bands, with a correlation coefficient of 0.96 and a mean absolute error of 4.5 m
426 (Fig. 6). This good correlation provides confidence about the spatial distribution of model
427 parameters.

428 Of the 10 adjusted parameters, unsaturated hydraulic conductivity and water content parameters
429 of alluvium and weathered bedrock had the strongest effect on the calibration and are, therefore,
430 well constrained by the measured streamflow and groundwater levels. These geologic features
431 represent the upper layers of the model domain and variations in their physical and hydraulic
432 properties control the rate of infiltration, evapotranspiration, drainage and, therefore, recharge. A

433 third parameter important in the calibration was the detention storage. This is because a
434 substantial amount of water from precipitation, especially at the beginning of the rainy season,
435 infiltrates without generating runoff events at the outfall (Fig. 5). This volume of water is controlled
436 not only by the properties of unsaturated zone (Table 2) but also by the value of detention storage
437 assigned to each land use class (Table 1). Conversely, alterations in rooting depth, LAI and crop
438 coefficient only resulted in small changes in streamflow. This is because significant runoff events
439 tend to occur during brief high-intensity precipitation events with a magnitude that far exceeds the
440 relative amount of evapotranspiration, which might occur during these events. For the same reason,
441 though, these factors had a relatively greater effect on the volume of water available for drainage
442 and subsequent recharge.

443
444 The ability of the model to simulate transient hydrologic conditions was also investigated through
445 the comparison between well hydrographs at five locations and the temporal variability of recharge
446 (Fig. 7). The recharge time series obtained from MIKE SHE (monthly time-step) ranges from 0.95
447 mm (November 2014) to 9.1 mm (March 2005). The latter is the response to the extraordinary
448 rainy season that occurred between December 2004 and March 2005 (903 mm) whereas the first is
449 due to dry conditions of the recent drought in California. The range of depth to groundwater from
450 1995 to 2014 at the five locations considered is 2.8–14.4 m at RD-09, 17.8–30 m at RD-35A, 16.2–
451 28.7 at RD-73, 37.7–50.8 m at RD-36B and 33.1–60.1 at WS-09B. The shape of these hydrographs
452 depends on surface (surface geology, topographic slope, land use) and subsurface (mechanisms of
453 flow in the vadose zone) factors. For our calibration purpose, it is noteworthy that, at all the
454 locations, the hydrographs show a good match with the recharge time series such that the peaks in
455 recharge coincide with water table rises. The greatest rises overlap the two highest recharge
456 periods (1998 and 2005), whereas a constant declining trend is observed from 2011 to 2014 in
457 response to drier conditions (Fig. 7). The good correlation suggests that, at this scale, the equivalent

458 porous media approach used is reasonable to simulate average responses in groundwater even
459 though the bedrock has many interconnected fractures.

460

461 *Spatial variability*

462 To study the spatial variability of the water budget components, average annual maps of infiltration
463 (Fig. 8Fig. 7a), evapotranspiration (Fig. 8Fig. 7b) and recharge (Fig. 8Fig. 7c) for the period 1995 -
464 2014 were created. Infiltration reflects the ability of water to enter the sub-surface, while recharge
465 represents the portion of infiltration that migrates through the evapotranspiration zone (ET zone)
466 toward the underlying water table.

467 Average infiltration for the catchment is 254 mm y⁻¹, corresponding to 64% of the total
468 precipitation but single cell values span over three orders of magnitude from 9 to > 1000 mm y⁻¹
469 (Fig. 8Fig. 7a). Low infiltration values are found in developed/paved (average 51 mm y⁻¹) and
470 massive-bedrock (average 14 mm y⁻¹) cells. Due to the low infiltration capacity, more runoff is
471 generated in these cells and, thus, infiltration is higher in nearby cells that receive the surface
472 water. Where these neighboring cells are covered by alluvium at the surface, infiltration is even
473 higher. On average, cells with alluvium at the surface have an infiltration value of 332 mm y⁻¹, 25%
474 more than those where bedrock outcrops. Higher infiltration is also displayed in depressed areas
475 such as those along the main drainages and where closed topographic depressions occur. These
476 cells collect most of the surface runoff creating conditions for focused infiltration and recharge.

477 Only a small portion of water that enters the subsurface reaches the water table because the
478 majority is lost due to evapotranspiration (Fig. 8Fig. 7b). The average evapotranspiration estimated
479 using MIKE SHE is 265 mm y⁻¹, a value slightly higher than the average infiltration. This excess of
480 ET over infiltration is attributed to canopy interception and evaporation of temporarily ponded
481 surface water. When removing these two water-loss processes, the average evapotranspiration is

482 237 mm y⁻¹, which corresponds to 60% of the annual precipitation and to 94% of the total
483 infiltration. Transpiration is the main process of ET contributing to about 70% of the total ET. This
484 result is expected considering the considerable depth of the roots (up to 5 meters for Chaparral)
485 and the fact that vegetation covers 83% of the catchment area. ~~As for the infiltration, s~~Single cell
486 values of ET span over three orders of magnitude, from 50 to >1000 mm y⁻¹. Since the actual
487 evapotranspiration depends strongly on the availability of subsurface water, the spatial variability
488 mimics the infiltration pattern and the two factors are strongly correlated (R²=0.84). Therefore, low
489 ET is associated with developed (~~asphalt, buildings~~) and massive bedrock areas and high ET values
490 are found along the main surface drainages where infiltration ~~water is collected to become~~is high
491 ~~and~~ locally available for evapotranspiration. The presence of alluvium at the surface increases the
492 ET values on average by 25%; for example, average ET in cells with chaparral and alluvium is 400
493 mm y⁻¹ whereas where chaparral is rooted in weathered bedrock is ~300 mm y⁻¹.

494 ~~The difference of infiltration and evapotranspiration maps (Fig. 8a and 7b8b), results in a~~ map of
495 the spatial distribution of the average annual recharge ~~is shown in (Fig. 8Fig. 7c)~~. The average
496 recharge value for the catchment is 16 mm y⁻¹ equal to 4.1 % of the precipitation and 6.5 % of the
497 infiltration. The range of variability of recharge is over three orders of magnitude and spatially
498 variable depending on topography, surface geology and land use. It is noteworthy that 79% of the
499 catchment has recharge less than 10 mm y⁻¹ and 90% less than 30 mm y⁻¹, which indicates that the
500 largest volumes of recharge are focused in small portions of the site. The recharge map (~~Fig. 8Fig.~~
501 ~~7c)~~ shows the influence of the surface parameters on recharge estimates. Recharge is high along the
502 main drainage because of the contribution of surface water flowing from the surrounding slopes
503 and enhanced infiltration where the topographic slope decreases abruptly. Relatively higher
504 recharge values are also observed in areas with alluvium at the surface because the infiltration and
505 retention capacities are higher and, therefore, water can seep from the overburden into the bedrock
506 once the evapotranspiration demand and driving forces are met. Recharge is also higher in cells

507 without vegetation cover, compared to other cells with equivalent topographic slope and surficial
508 geology, because the evapotranspiration in these areas is lower.

509

510 *Temporal variability*

511 The seasonal variability of the hydrologic processes was examined analyzing unsaturated water
512 budgets at two locations with different land use and surficial geology (UZ-1 and UZ-2 in Fig.1)

513 Among the 20 years, we show the monthly average daily values from 2005 to 2007. This time span
514 features a wet year (2005 – 978 mm), a dry year (2007 – 149 mm) and one year with average
515 precipitation (2006 - 331 mm) and therefore is reasonably representative of the simulated period.

516 For areas with bedrock outcrop not covered by vegetation (UZ-1 in Fig. 1), the infiltration ranges
517 from 0 to 2.5 mm d⁻¹ (Fig. 9 Fig. 8). The infiltration pattern shows null or minimal values during the
518 summer and positive events during the wet season. Water that enters the subsurface between April
519 and January replenishes the water content in the ET zone and becomes available for evaporation
520 but not for drainage. Evaporation is null during the summer because of the lack of precipitation
521 and because all the water stored in the first 20 cm of bedrock has been taken up by evaporation in
522 the previous months. Downward flux at the bottom of the ET zone (i.e. drainage) only happens
523 episodically when the water content in the ET zone is above the field capacity, at the end of the wet
524 season (i.e., March and April) or occasionally after exceptionally high-intensity precipitation events
525 (i.e., January 2005).

526 For areas with alluvium at surface (UZ-2 in Fig. 1) the infiltration has the same pattern but a
527 different order of magnitude (from 0 to 30 mm d⁻¹) due to the higher infiltration capacity of the
528 alluvium (Fig. 9 Fig. 8). Here, the available water capacity of the ET zone is greater because of the
529 different physical properties (e.g. larger porosity) of the soil and the greater depth of the ET zone.
530 Therefore, almost all the infiltration water is taken up by the evapotranspiration. Unlike areas

531 without vegetation, evapotranspiration is not directly related to precipitation events and occurs
532 more continuously throughout the year. This is because alluvium stores a greater volume of water
533 in the ET zone that is nearly completely consumed by ET. A drainage flux is observed only during
534 high-intensity precipitation events that create near-saturation conditions such that water cannot be
535 held by tension in the shallow unsaturated zone and downward flow is initiated.

536 For both cases, drainage is not steady throughout the year but occurs episodically, controlled by
537 antecedent soil water content in the ET zone and by the intensity of precipitation. During drier-
538 than-average years, such as 2007, drainage occurs in areas without vegetation, whereas no
539 drainage is observed in cells with vegetation cover. After crossing the bottom of the ET zone, water
540 arrives at the water table with a time lag depending on the magnitude of the flux and on the
541 physical properties and the thickness of the vadose zone.

542 *Model validation*

543 ~~The validation of the model requires comparison of the simulation results to other evidence,~~
544 ~~independent of those used in the calibration.~~

545 The ability of the model to simulate transient hydrologic conditions was investigated through the
546 comparison between well hydrographs at five locations and the temporal variability of recharge
547 (Fig. 9). The spatially-average recharge rates obtained from MIKE SHE (monthly time-step) range
548 from 0.95 mm (November 2014) to 9.1 mm (March 2005). The latter is the response to the
549 extraordinary rainy season that occurred between December 2004 and March 2005 (903 mm)
550 whereas the first is due to dry conditions of the recent drought in California. The range of depth to
551 groundwater from 1995 to 2014 at the five locations considered is 2.8 – 14.4 m at RD-09, 17.8 – 30
552 m at RD-35A, 16.2 – 28.7 at RD-73, 37.7 – 50.8 m at RD-36B and 33.1 – 60.1 at WS-09B. The shape
553 of these hydrographs depends on surface (surface geology, topographic slope, land use) and
554 subsurface (mechanisms of flow in the vadose zone) conditions. For our validation purpose, it is

555 noteworthy that, at all the locations, the hydrographs show a good match with the recharge time
556 series such that the peaks in recharge coincide with water table rises. The greatest rises overlap the
557 two highest recharge periods (1998 and 2005), whereas a constant declining trend is observed
558 from 2011 to 2014 in response to drier conditions (Fig. 9). The good correlation suggests that, at
559 this scale, the equivalent porous media approach used is reasonable to simulate average responses
560 in groundwater because, although the bedrock has many interconnected fractures, it is only a minor
561 contributor to recharge.

562 The average recharge value for the catchment from the simulation is 16 mm y^{-1} and is consistent
563 with previous recharge estimates obtained for the site using the CMB method (19 mm y^{-1} – 4.2% of
564 the average precipitation, Manna et al., 2016; 16 mm y^{-1} – 3.5% of the average precipitation, Manna
565 et al., 2017), ~~for other sandstone aquifers in semi-arid areas in the United States (Heilweil et al.,~~
566 ~~2006) and for other study areas in semi-arid regions around the world (0.2 – 35 mm y^{-1} equal to 0 –~~
567 ~~5% of the average precipitation, Scanlon et al., 2006).~~ Interestingly, ~~t~~he frequency distribution of
568 recharge values from the MIKE SHE simulation (92% of the domain has average recharge lower
569 than 40 mm y^{-1}) also corresponds well to the range of variability based on chloride (from 0 to 43
570 mm y^{-1}) reported by Manna et al. (2016) and Manna et al. (2017). ~~This represents a mutual~~
571 ~~validation of the two approaches, based on independent datasets and for different timescales.~~

572 For additional information on recharge processes, we analyzed water isotopes obtained from
573 rainfall and groundwater samples (Fig. 10). The samples show a substantial isotopic range from
574 one precipitation event to another over the one-year collection period. ^{18}O varies between -2.8 and
575 -12.1‰ for B/886 and -2.8 and -11.7‰ for RDMF and ^2H varying between -11 and -89‰ for B/886
576 and -12 and -85‰ for RDMF (Table 3). This large range of values is probably due to the two
577 different trajectories of the precipitation events in southern California, one originating in the Pacific
578 and one over the Gulf of Mexico, as found by Friedman et al. (1992). The volume weighted mean

579 values for the two stations are -8.2 and -54.2‰ for B/886 and -8.2 and -56.2‰ for RDMF and are
580 consistent with global-scale maps of water isotopes for precipitation in southern California (Bowen
581 and Revenaugh, 2003).

582 Unlike rainfall, groundwater samples fall within a narrower range: from -6.5 to -7.5‰ for ^{18}O and
583 from -40.2 and to -52.2‰ for ^2H . All the samples are aligned along the local meteoric water line
584 (Fig. 10) ~~suggesting indicating~~ little if any evaporation from standing water on surface. This lack of
585 concentration effect on the isotopes is apparently in contrast to the chloride data. finding contrasts
586 ~~the results of~~ Manna et al. (2016) ~~who~~ found that Cl concentrations in groundwater are, on average,
587 20 times greater those from atmospheric deposition because of the strong influence of
588 evapotranspiration. The common explanation for the lack of evaporation effects on the water
589 isotopes is in groundwater is that the transpiration is the main evapotranspiration process (Clark,
590 2015; Cook and Böhlke, 2000). Although it transpiration through the vegetation causes a
591 concentration effect on Cl, ~~transpiration through vegetation, it~~ does not cause fractionation of the
592 water isotopes and therefore the groundwater samples are not enriched (Clark, 2015; Cook and
593 Böhlke, 2000).

594 The lack of evaporative water isotope signature associated with high groundwater Cl concentration
595 ~~in porewater~~ can also be explained by recharging water that ~~quickly~~ crosses the ET zone mobilizing
596 precipitated salts but without any evaporation. This hypothesis supports the results of the MIKE
597 SHE simulations, which show that throughout the year there are only episodic fluxes at the bottom
598 of the ET zone (Fig. 9). A relevant observation that corroborates this hypothesis is that the isotopic
599 composition of groundwater is similar to that found in rainfall samples collected at the end of the
600 wet season (March and June) or, on occasion, with high-intensity precipitation events (January -
601 203 mm) (Table 3). This similarity can be attributed to the preponderance of recharge occurring at
602 these times and thereby resulting in the groundwater values being different from the weighted

603 ~~mean precipitation a selective recharge mechanism that causes groundwater to have isotopic~~
604 ~~composition different by 1.2‰ ¹⁸O and 3‰ ²H, from the weighted mean of precipitation and~~
605 ~~similar to that of the rainfall that episodically crosses the ET zone.~~ This proposed model of episodic
606 ~~fast~~ flow through the unsaturated ET zone is also corroborated by the evidence presented by
607 Manna et al., (2017) that, on average, 20% of the flow in the vadose zone occurs as fast flow
608 through the interconnected fractured network.

609

610 Discussion and Conceptual model for recharge

611 To summarize the findings of this study, and its relationship to the literature and to the previous
612 recharge studies at the site (Manna et al., 2016; Manna et al., 2017), we propose the following
613 process-based conceptual model for site recharge (Fig. 11).

614 The average recharge value is 16 mm y⁻¹ which is consistent with previous estimates at the site, and
615 with those obtained for other sandstone aquifers in semi-arid areas in the United States (4% -
616 Heilweil et al., 2006) and other studies in semi-arid regions around the world (0.2 – 35 mm y⁻¹ equal
617 to 0 – 5% of the average precipitation, Scanlon et al., 2006). Recharge varies greatly across the
618 catchment as a function of topography, surface geology, and land use. High recharge occurs where
619 most runoff water seeps into the subsurface, creating conditions for focused recharge. This
620 condition happens where closed depressions occur and where sloped topography abruptly
621 transitions to flat along the main surface drainages (Fig. 11a). Here, in most areas, alluvium covers
622 the fractured porous bedrock, thus enhancing infiltration and temporary storage of infiltrated
623 water. Generally, in semiarid regions, The high recharge values along the valley, at the edge of the
624 slope might recall referred to what has been defined as Mountain Front Recharge (MFR) (Wilson
625 and Guan, 2004). However, our catchment is located on the top of a ridge standing 300 m above the
626 surrounding valleys (Manna et al., 2016) and, thus, our case study represents groundwater

627 [recharge on the mountain block rather than MFR. Nonetheless, it is interesting that the processes](#)
628 [observed in our small catchment are similar to those described in for aquifer-scale recharge studies](#)
629 (Aishlin and McNamara, 2011; Carling et al., 2012; Manning and Solomon, 2003; Bresciani et al.,
630 2018) [-and defined as MFR.](#)

631 -Infiltration from April to December (dry season) contributes to replenish the water content in the
632 ET zone and remains available for evapotranspiration (Fig. 11b). Conversely, during the wet season,
633 infiltration crosses the bottom of the ET zone (i.e. drainage) and migrates deeper through the
634 vadose zone. This happens when the soil is above the field capacity (FC), which is more frequent at
635 the end of the wet season in March or April and/or during high-intensity precipitation events, (Fig.
636 11c). This recharging water quickly crosses the ET zone, as shown by the ET zone water budgets
637 extracted from MIKE SHE (Fig. 9), and by the lack of evaporative signature in isotope composition
638 (Fig. 10).

639 The occurrence of this fast/preferential flow out of the ET zone is also corroborated by the analysis
640 of vertical chloride porewater concentration profiles in the unsaturated zone (Manna et al., 2017).
641 The Cl concentration is high in the ET zone (up to 10,000 mg L⁻¹) and considerably lower in deeper
642 vadose and groundwater zones (average 49 mg L⁻¹). The higher Cl concentrations in the shallow
643 subsurface is the effect of strong evapotranspiration that takes up water but not chloride, whereas
644 the lower concentration below is due to fast/preferential flow of water that escapes the
645 concentrating effect of water loss in the shallower zone. [Similar case studies showing similar](#)
646 [results for of water that crosses the ET zone preferentially in time and space to become potentially](#)
647 [recharge have been also reported in literature](#) (Kurtzman et al., 2016). [also referred to as selective](#)
648 [recharge](#) (Gat and Tzur, 1967; Florea, 2013; Krabbenhoft et al., 1990). [The occurrence of these](#)
649 [fluxes has been also analyzed in function of precipitation characteristics and antecedent water](#)
650 [content with rainfall intensity being the main factor](#) (Allocca et al., 2015; Crosbie et al., 2012; Nasta
651 et al., 2018; Taylor et al., 2013).

652 Upon reaching the deeper vadose zone, water is redistributed between intergranular matrix flow
653 and fracture flow due to wettability and saturation concepts. The fractures and the matrix pores
654 drain the water from the ET zone. Active flow through the fractures is possible under conditions
655 such as ponding or intense precipitation, when a continuous slug of water lets i) the advective front
656 move ahead into the fracture (1 in Fig. 11c); ii) the matrix water flow into the fractures (2 in Fig.
657 11c). Otherwise, water is drawn from the fractures into the unsaturated matrix blocks (3 in Fig.
658 11c) and contributes to the slow vertical intergranular matrix flow (4 in Fig. 11c). According to
659 Manna et al. (2017), the first two mechanisms are much less frequent and contribute, on average, to
660 only 20% of the total recharge. It is most likely that conditions for flow in the fractures occur
661 episodically in areas of the site with high infiltration (topographic low and alluvium at the surface)
662 where temporary perched systems are observed.

663

664 **Conclusions**

665 ~~This is the first study to combine MIKE SHE simulations supported by analysis of water isotopes~~
666 ~~and chloride mass balance to assess recharge in a semi-arid region.~~ For the upland bedrock
667 catchment, the surface water-groundwater numerical model (MIKE SHE), using a fine numerical
668 grid (20 ×20 m) with calibration to streamflow and groundwater levels, simulated the spatial and
669 temporal variability of recharge ~~at a study across a 2.16 km² catchment site in a semi-arid region of~~
670 southern California, USA. ~~This is the first study that combined MIKE SHE simulations supported by~~
671 ~~analysis of water isotopes and chloride mass balance to assess recharge in a sedimentary bedrock~~
672 ~~aquifer in a semi-arid region. The calibrated S_s simulations, indeed,~~ were judged to be reliable and
673 strongly reflective of the natural system, based on the validation comparisons to mean recharge
674 values obtained independently from the chloride mass balance method (Manna et al., 2016; Manna
675 et al., 2017) and ~~comparisons~~ to the timing of major recharge events indicated by water isotopes

676 and water level fluctuations. The simulations showed that major flux events at the bottom of the
677 evapotranspiration zone, that result in recharge tens of meters below the surface, occur
678 episodically mostly only at the end of the rainy season and that recharge varies across the
679 catchment between 0 and 1000 mm y⁻¹. The fine numerical grid in the horizontal plane allowed
680 meaningful examination of recharge spatial variability. A substantially coarser grid would obscure
681 influences of key surface features on the hydrologic processes. ~~This is the first study to combine~~
682 ~~MIKE SHE simulations supported by analysis of water isotopes and chloride mass balance to assess~~
683 ~~recharge in a semi-arid region.~~

684 The results obtained from the catchment-scale simulations (2.16 km² area) will be used to
685 specify rules for recharge to be assigned to the upper boundary condition of a 3-D site-wide
686 numerical EPM groundwater flow model (FeFlow52 km² area), covering the studied catchment and
687 a much larger area beyond (52 km²). The modeled groundwater domain has many contaminant
688 plumes and recharge is key to determine the fluxes available to transport contaminants.
689 ~~to determine the distribution of recharge affecting groundwater flow in the fractured bedrock.~~
690 ~~Many contaminant source zones and plumes occur in the rock where the variable recharge and~~
691 ~~groundwater fluxes are a major governing factor on plume migration.~~

692 The aim of the MIKE SHE model It is important to highlight that our modeling aimed to represent
693 the natural hydrologic conditions, after site industrial operations ceased nearly more than a
694 decade ago. During historical operations from 1950's through mid-2000's, use of imported and
695 pumped groundwater in specific areas likely caused increases to infiltration and recharge locally in
696 some areas. These conditions are beyond the scope of this paper but worth further consideration in
697 a follow-on study as it relates to land use changes when contaminant releases occurred and may
698 provide insights regarding how contaminant migration rates may have been influenced. Future
699 modeling efforts will also evaluate the effect on recharge of the surface water control systems

700 currently in place on the site. These storm water management measures aim to limit the volume of
701 water leaving the catchment and, therefore, will likely influence the natural rates of the other
702 hydrologic processes.

703

704 **Acknowledgements**

705 Funding for this work was provided by an NSERC Industrial Research Chair (n. IRCPJ 363783) to
706 Professor Beth Parker in partnership with the Boeing Company. Field work was supported by
707 the site owner, their consultants (MWH Inc., now Stantec), and University of Guelph colleagues,
708 especially Amanda Pierce from the G³⁶⁰ Institute for Groundwater Research, who collected and
709 analyzed isotope samples.

710

711

712 **References**

713 Aishlin, P., and McNamara, J. P.: Bedrock infiltration and mountain block recharge accounting using
714 chloride mass balance, *Hydrological Processes*, 25, 1934-1948, 2011.

715 Allegre, V., Brodsky, E. E., Xue, L., Nale, S. M., Parker, B. L., and Cherry, J. A.: Using earth-tide induced
716 water pressure changes to measure in situ permeability: A comparison with long-term pumping
717 tests, *Water Resources Research*, 52, 3113-3126, 10.1002/2015wr017346, 2016.

718 Allen, R. G., Pereira, L. S., Raes, D., and Smith, M.: Crop evapotranspiration-Guidelines for computing
719 crop water requirements-FAO Irrigation and drainage paper 56, Fao, Rome, 300, D05109, 1998.

720 Allocca, V., De Vita, P., Manna, F., and Nimmo, J. R.: Groundwater recharge assessment at local and
721 episodic scale in a soil mantled perched karst aquifer in southern Italy, *Journal of Hydrology*, 529,
722 843-853, 10.1016/j.jhydrol.2015.08.032, 2015.

723 AquaResource, and MWH: Three-Dimensional Groundwater Flow Model Report. Santa Susana Field
724 Laboratory., 2007.

725 Bowen, G. J., and Revenaugh, J.: Interpolating the isotopic composition of modern meteoric
726 precipitation, *Water Resources Research*, 39, 2003.

727 Bresciani, E., Cranswick, R. H., Banks, E. W., Batlle-Aguilar, J., Cook, P. G., and Batelaan, O.: Using
728 hydraulic head, chloride and electrical conductivity data to distinguish between mountain-front and
729 mountain-block recharge to basin aquifers, *Hydrology & Earth System Sciences*, 22, 2018.

730 Canadell, J., Jackson, R. B., Ehleringer, J. R., Mooney, H. A., Sala, O. E., and Schulze, E. D.: Maximum
731 rooting depth of vegetation types at the global scale, *Oecologia*, 108, 583-595,
732 10.1007/bf00329030, 1996.

733 Carling, G. T., Mayo, A. L., Tingey, D., and Bruthans, J.: Mechanisms, timing, and rates of arid region
734 mountain front recharge, *Journal of hydrology*, 428, 15-31, 2012.

735 Cartwright, I., Weaver, T. R., Stone, D., and Reid, M.: Constraining modern and historical recharge
736 from bore hydrographs, H-3, C-14 and chloride concentrations: Applications to dual-porosity
737 aquifers in dryland salinity areas, Murray Basin, Australia, *Journal of Hydrology*, 332, 69-92,
738 10.1016/j.jhydrol.2006.06.034, 2007.

739 Cherry J.A., P. B. L., McWhorter D.: Site conceptual model for the migration and fate of contaminants
740 in groundwater at the Santa Susana Field Laboratory, Simi Valley, California., 2009.

741 Cherry, J. A., McWorther, D. B., and Parker, B. L.: Site conceptual model for the migration and fate of
742 contaminants in groundwater at the Santa Susana Field Laboratory, Simi, California (draft), vols 1-
743 4, Association with the University of Guelph, Toronto, ON; MWH, Walnut Creek, CA, 2009.

744 Chin, D. A., Mazumdar, A., and Roy, P. K.: Water-resources engineering, Prentice Hall Englewood
745 Cliffs, 2000.

746 Cilona, A., Aydin, A., and Johnson, N.: Permeability of a fault zone crosscutting a sequence of
747 sandstones and shales and its influence on hydraulic head distribution in the Chatsworth
748 Formation, California, USA, Hydrogeology Journal, 23, 405-419, 10.1007/s10040-014-1206-1,
749 2015.

750 Cilona, A., Aydin, A., Likerman, J., Parker, B., and Cherry, J.: Structural and statistical characterization
751 of joints and multi-scale faults in an alternating sandstone and shale turbidite sequence at the Santa
752 Susana Field Laboratory: Implications for their effects on groundwater flow and contaminant
753 transport, Journal of Structural Geology, 85, 95-114, 10.1016/j.jsg.2016.02.003, 2016.

754 CIMIS: Reference Evapotranspiration. Department of Land Arid and Water Resources, University of
755 California, Davis and Water Efficiency Office, California Department of Water Resources, California
756 Irrigation Management Unit., 1999.

757 Clark, I.: Groundwater geochemistry and isotopes, CRC press, 2015.

758 Coelho, V. H. R., Montenegro, S., Almeida, C. N., Silva, B. B., Oliveira, L. M., Gusmão, A. C. V., Freitas, E.
759 S., and Montenegro, A. A.: Alluvial groundwater recharge estimation in semi-arid environment using
760 remotely sensed data, *Journal of Hydrology*, 548, 1-15, 2017.

761 Cook, P. G., and Böhlke, J.-K.: Determining timescales for groundwater flow and solute transport, in:
762 *Environmental tracers in subsurface hydrology*, Springer, 1-30, 2000.

763 Crosbie, R. S., McCallum, J. L., Walker, G. R., and Chiew, F. H.: Episodic recharge and climate change
764 in the Murray-Darling Basin, Australia, *Hydrogeology Journal*, 20, 245-261, 2012.

765 Crosbie, R. S., Davies, P., Harrington, N., and Lamontagne, S.: Ground truthing groundwater-recharge
766 estimates derived from remotely sensed evapotranspiration: a case in South Australia,
767 *Hydrogeology Journal*, 23, 335-350, 10.1007/s10040-014-1200-7, 2015.

768 Crosbie, R. S., Peeters, L. J., Herron, N., McVicar, T. R., and Herr, A.: Estimating groundwater recharge
769 and its associated uncertainty: Use of regression kriging and the chloride mass balance method,
770 *Journal of Hydrology*, 561, 1063-1080, 2018.

771 Davis, F., Stoms, D., Hollander, A., Thomas, K., Stine, P., Odion, D., Borchert, M., Thorne, J., Gray, M.,
772 and Walker, R.: The California gap analysis project–final report. University of California, Santa
773 Barbara, CA, 1998.

774 De Vries, J. J., and Simmers, I.: Groundwater recharge: an overview of processes and challenges,
775 *Hydrogeology Journal*, 10, 5-17, 2002.

776 Doherty, J.: PEST model-independent parameter estimation user manual, Watermark Numerical
777 Computing, Brisbane, Australia, 3338, 3349, 2004.

778 Flint, A. L., Flint, L. E., Bodvarsson, G. S., Kwicklis, E. M., and Fabryka-Martin, J.: Evolution of the
779 conceptual model of unsaturated zone hydrology at Yucca Mountain, Nevada, *Journal of Hydrology*,
780 247, 1-30, 2001.

781 Flint, L. E., and Flint, A. L.: Regional analysis of ground-water recharge, *Ground-water recharge in*
782 *the arid and semiarid southwestern United States*, 29-59, 2007.

783 Florea, L. J.: Selective recharge and isotopic composition of shallow groundwater within temperate,
784 epigenic carbonate aquifers, *Journal of hydrology*, 489, 201-213, 2013.

785 Friedman, I., Smith, G. I., Gleason, J. D., Warden, A., and Harris, J. M.: Stable isotope composition of
786 waters in southeastern California 1. Modern precipitation, *Journal of Geophysical Research:*
787 *Atmospheres*, 97, 5795-5812, 1992.

788 Gat, J., and Tzur, Y.: Modification of the isotopic composition of rainwater by processes which occur
789 before groundwater recharge, *Isotopes in hydrology. Proceedings of a symposium*, 1967,

790 Gebru, T. A., and Tesfahunegn, G. B.: Chloride mass balance for estimation of groundwater recharge
791 in a semi-arid catchment of northern Ethiopia, *Hydrogeology Journal*, 1-16, 2018.

792 Heilweil, V. M., Solomon, D. K., and Gardner, P. M.: Borehole environmental tracers for evaluating
793 net infiltration and recharge through desert bedrock, *Vadose Zone Journal*, 5, 98-120, 2006.

794 Hernández-Marín, M., Guerrero-Martínez, L., Zermeño-Villalobos, A., Rodríguez-González, L.,
795 Burbey, T. J., Pacheco-Martínez, J., Martínez-Martínez, S. I., and González-Cervantes, N.: Spatial and
796 temporal variation of natural recharge in the semi-arid valley of Aguascalientes, Mexico,
797 *Hydrogeology Journal*, 26, 2811-2826, 2018.

798 Huang, Y., Chang, Q., and Li, Z.: Land use change impacts on the amount and quality of recharge
799 water in the loess tablelands of China, *Science of the Total Environment*, 628, 443-452, 2018.

800 ITRC: California Crop and Soil Evapotranspiration, ITRC Report No. R 03-001. 2003.

801 Jebreen, H., Wohnlich, S., Wisotzky, F., Banning, A., Niedermayr, A., and Ghanem, M.: Recharge
802 estimation in semi-arid karst catchments: Central West Bank, Palestine, *Grundwasser*, 23, 91-101,
803 2018.

804 Krabbenhoft, D. P., Bowser, C. J., Anderson, M. P., and Valley, J. W.: Estimating groundwater
805 exchange with lakes: 1. The stable isotope mass balance method, *Water Resources Research*, 26,
806 2445-2453, 1990.

807 Kristensen, K., and Jensen, S.: A model for estimating actual evapotranspiration from potential
808 evapotranspiration, *Hydrology Research*, 6, 170-188, 1975.

809 Kurtzman, D., Baram, S., and Dahan, O.: Soil-aquifer phenomena affecting groundwater under
810 vertisols: a review, *Hydrology and Earth System Sciences*, 20, 1-12, 2016.

811 Levy, Y., Shapira, R. H., Chefetz, B., and Kurtzman, D.: Modeling nitrate from land surface to wells'
812 perforations under agricultural land: success, failure, and future scenarios in a Mediterranean case
813 study, *Hydrology & Earth System Sciences*, 21, 2017.

814 Li, Z., Chen, X., Liu, W., and Si, B.: Determination of groundwater recharge mechanism in the deep
815 loessial unsaturated zone by environmental tracers, *Science of the Total Environment*, 586, 827-
816 835, 2017.

817 Link, M. H., Squires, R. L., and Colburn, I. P.: Slope and deep-sea fan facies and paleogeography of
818 Upper Cretaceous Chatsworth Formation, Simi Hills, California, *AAPG Bulletin*, 68, 850-873, 1984.

819 Liu, H.-L., Chen, X., Bao, A.-M., and Wang, L.: Investigation of groundwater response to overland flow
820 and topography using a coupled MIKE SHE/MIKE 11 modeling system for an arid watershed,
821 *Journal of Hydrology*, 347, 448-459, 2007.

822 Ma, L., He, C., Bian, H., and Sheng, L.: MIKE SHE modeling of ecohydrological processes: Merits,
823 applications, and challenges, *Ecological Engineering*, 96, 137-149, 2016.

824 Manna, F., Cherry, J. A., McWhorter, D. B., and Parker, B. L.: Groundwater recharge assessment in an
825 upland sandstone aquifer of southern California, *Journal of Hydrology*, 541, 787-799,
826 10.1016/j.jhydrol.2016.07.039, 2016.

827 Manna, F., Walton, K. M., Cherry, J. A., and Parker, B. L.: Mechanisms of recharge in a fractured
828 porous rock aquifer in a semi-arid region, *Journal of Hydrology*, 555, 869-880,
829 10.1016/J.Jhydrol.2017.10.060, 2017.

830 Manning, A. H., and Solomon, D. K.: Using noble gases to investigate mountain-front recharge,
831 Journal of Hydrology, 275, 194-207, 2003.

832 MWH: Draft-site wide groundwater remedial investigation report Santa Susana Field Laboratory,
833 Ventura County, California. Prepared for The Boeing Company, NASA and U.S. DOE by MWH Global
834 Inc., Walnut Creek, CA., 2009.

835 MWH: Hydrogeological Characterization of Faults. Santa Susana Field Laboratory, Ventura County,
836 Ca. Prepared for The Boeing Company by Dr. Nicholas M. Johnson, MWH Americas Inc., 2121 N.
837 California Blvd., Suite 600, Walnut Creek, CA 94596., 2016.

838 Nasta, P., Adane, Z., Lock, N., Houston, A., and Gates, J. B.: Links between episodic groundwater
839 recharge rates and rainfall events classified according to stratiform-convective storm scoring: A
840 plot-scale study in eastern Nebraska, Agricultural and Forest Meteorology, 259, 154-161, 2018.

841 Pierce, A. A., Chapman, S. W., Zimmerman, L. K., Hurley, J. C., Aravena, R., Cherry, J. A., and Parker, B.
842 L.: DFN-M field characterization of sandstone for a process-based site conceptual model and
843 numerical simulations of TCE transport with degradation, Journal of contaminant hydrology, 212,
844 96-114, 2018a.

845 Pierce, A. A., Parker, B. L., Ingleton, R., and Cherry, J. A.: Novel Well Completions in Small Diameter
846 Coreholes Created Using Portable Rock Drills, Groundwater Monitoring & Remediation, 38, 42-55,
847 2018b.

848 Quinn, P., Cherry, J. A., and Parker, B. L.: Combined use of straddle packer testing and FLUTE
849 profiling for hydraulic testing in fractured rock boreholes, *Journal of Hydrology*, 524, 439-454,
850 2015.

851 Quinn, P. M., Cherry, J. A., and Parker, B. L.: Depth-discrete specific storage in fractured sedimentary
852 rock using steady-state and transient single-hole hydraulic tests, *Journal of Hydrology*, 542, 756-
853 771, 2016.

854 Refsgaard, C.: Mike she, *Computer models of catchment hydrology*, 809-846, 1995.

855 Richards, L. A.: Capillary conduction of liquids through porous mediums, *physics*, 1, 318-333, 1931.

856 Scanlon, B. R.: Uncertainties in estimating water fluxes and residence times using environmental
857 tracers in an arid unsaturated zone, *Water Resources Research*, 36, 395-409, 2000.

858 Scanlon, B. R., Keese, K. E., Flint, A. L., Flint, L. E., Gaye, C. B., Edmunds, W. M., and Simmers, I.: Global
859 synthesis of groundwater recharge in semiarid and arid regions, *Hydrological Processes: An*
860 *International Journal*, 20, 3335-3370, 2006.

861 Scanlon, B. R., Reedy, R. C., and Tachovsky, J. A.: Semiarid unsaturated zone chloride profiles:
862 Archives of past land use change impacts on water resources in the southern High Plains, United
863 States, *Water Resources Research*, 43, 2007.

864 Scurlock, J., Asner, G., and Gower, S.: Worldwide historical estimates of leaf area index, 1932–2000,
865 ORNL/TM-2001/268, 34, 2001.

866 Smerdon, B., Allen, D., Grasby, S., and Berg, M.: An approach for predicting groundwater recharge in
867 mountainous watersheds, *Journal of Hydrology*, 365, 156-172, 2009.

868 Sterling, S., Parker, B., Cherry, J., Williams, J., Lane Jr, J., and Haeni, F.: Vertical cross contamination of
869 trichloroethylene in a borehole in fractured sandstone, *Groundwater*, 43, 557-573, 2005.

870 Sukhija, B., Reddy, D., Nagabhushanam, P., and Hussain, S.: Recharge processes: piston flow vs
871 preferential flow in semi-arid aquifers of India, *Hydrogeology Journal*, 11, 387-395, 2003.

872 Taylor, R. G., Todd, M. C., Kongola, L., Maurice, L., Nahozya, E., Sanga, H., and MacDonald, A. M.:
873 Evidence of the dependence of groundwater resources on extreme rainfall in East Africa, *Nature*
874 *Climate Change*, 3, 374, 2013.

875 Turkeltaub, T., Kurtzman, D., Russak, E., and Dahan, O.: Impact of switching crop type on water and
876 solute fluxes in deep vadose zone, *Water Resources Research*, 51, 9828-9842, 2015.

877 Van Genuchten, M. T.: A closed-form equation for predicting the hydraulic conductivity of
878 unsaturated soils 1, *Soil science society of America journal*, 44, 892-898, 1980.

879 Wang, H., Kgotlhang, L., and Kinzelbach, W.: Using remote sensing data to model groundwater
880 recharge potential in Kanye region, Botswana, 2008.

881 Wheeler, H., Sorooshian, S., and Sharma, K. D.: *Hydrological modelling in arid and semi-arid areas*,
882 Cambridge University Press, 2007.

883 Wilson, J. L., and Guan, H.: Mountain-block hydrology and mountain-front recharge, Groundwater
884 recharge in a desert environment: The Southwestern United States, 9, 2004.

885 Wood, W. W., and Sanford, W. E.: Chemical and isotopic methods for quantifying ground-water
886 recharge in a regional, semiarid environment, Groundwater, 33, 458-468, 1995.

887 Xie, Y., Cook, P. G., Simmons, C. T., Partington, D., Crosbie, R., and Batelaan, O.: Uncertainty of
888 groundwater recharge estimated from a water and energy balance model, Journal of Hydrology,
889 561, 1081-1093, 2018.

890

891

892

893

894

895

896

897

898

899 *Table 1 Land use class-specific parameters to model runoff and evapotranspiration. The values are based on literature: 1*
900 *Canadell et al., 1996; 2 Scurlock et al., 2001; 3 Chin et al., 2006.*

Land Use Class	Surface roughness (Manning's n) ¹	Detention storage (mm) ¹	Leaf Area Index ²	Depth of the evapotranspiration zone (m) ³
Developed*	0.04	1	-	0.2

Coastal Scrub	0.2	7.5	1.8 - 3	1.8 - 3
Chaparral	0.2	7.5	2.8 - 4.5	3.1 - 5
Exposed Bedrock/ Massive bedrock*	0.05	3	-	0.2

907

908

909

910

911 *Table 2 Saturated hydraulic conductivity (ks) of the different hydrogeologic units.*

Hydrogeologic unit	K_s ($m\ s^{-1}$)
Alluvium	1×10^{-6}
Weathered bedrock	2×10^{-7}
Unweathered bedrock	1×10^{-10} to 1×10^{-5}
Unweathered bedrock	4.1×10^{-10} to 2.3×10^{-7}
Unweathered bedrock	1×10^{-9} to 1×10^{-6}

Van Genuchten parameters

Hydrogeologic unit	Lithology	K_s ($m\ s^{-1}$)	Saturation (θ_s)	Field capacity (θ_{fc})	Residual Water content (θ_{fer})	α	n	l
Alluvium		1×10^{-6}	0.4	0.25	0.05	0.021	1.61	0.5
Weathered bedrock		2×10^{-7}	0.2	0.11	0.01	0.033	1.49	0.5
Unweathered bedrock	Shale/Siltstone	4.1×10^{-10} to 2.3×10^{-7}	0.13	0.1	0.025	0.01	1.23	0.5
Unweathered bedrock	Sandstone	1×10^{-10} to 1×10^{-5}	0.13	0.09	0.01	0.01	2	0.5
Unweathered bedrock	Fault zone	1×10^{-9} to 1×10^{-6}	0.13	0.1	0.025	0.01	2	0.5

912

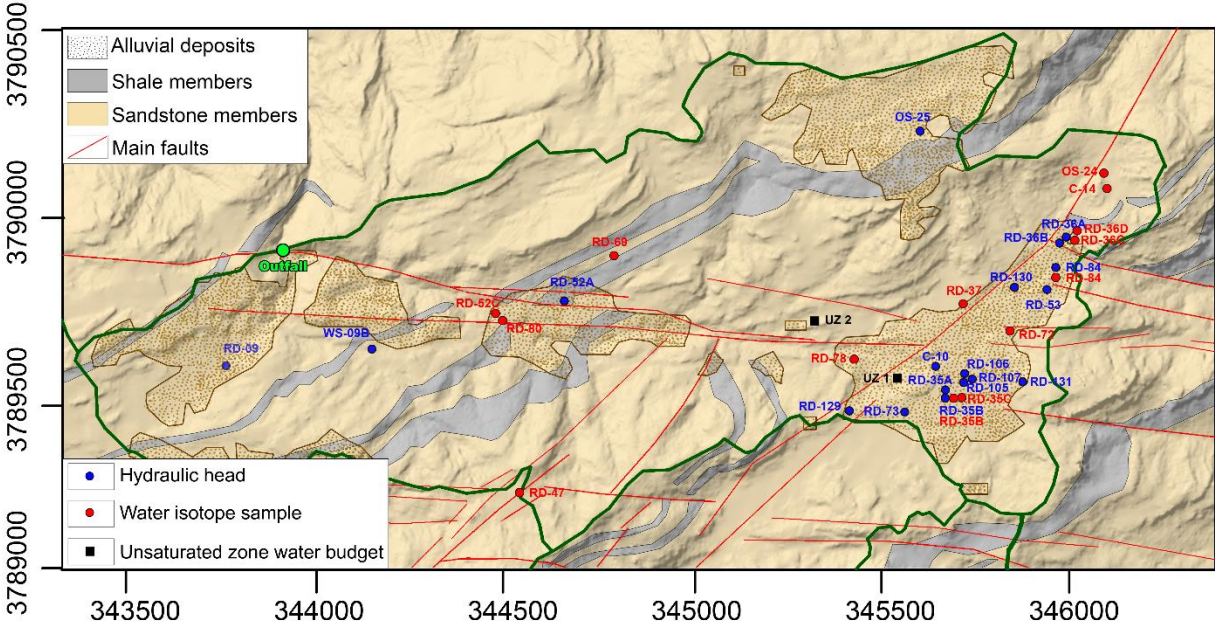
929
930
931
932
933
934
935
936
937
938
939
940
941
942
943
944

Table 3 Stable isotope composition of rainfall.

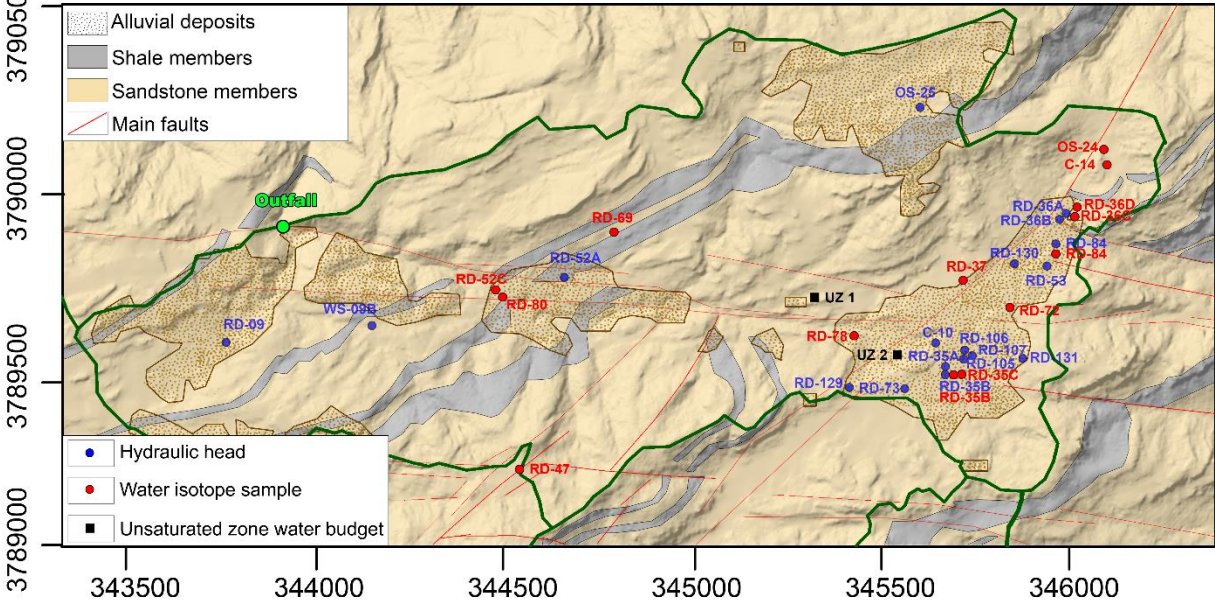
Date	B/886 Rain Gauge			RMDF Rain Gauge			Average		
	$\delta^{18}\text{O}$	$\delta^2\text{H}$	Rainfall (mm)	$\delta^{18}\text{O}$	$\delta^2\text{H}$	Rainfall (mm)	$\delta^{18}\text{O}$	$\delta^2\text{H}$	Rainfall (mm)
4/10/1994	-4	-19	3				-4.0	-19.0	3
25/11/1994	-5.2	-18	6	-5.1	-16	6	-5.2	-17.0	6
13/12/1994	-5.4	-23	9	-5.4	-25	9	-5.4	-24.0	9
24/12/1994	-10.3	-77	18	-10.1	-69	18	-10.2	-73.0	18
4/1/1995	-10.3	-75	94	-9.9	-69	121	-10.1	-72.0	108
11/1/1995	-6	-33	205	-7.4	-45	202	-6.7	-39.0	203
13/01/1995	-4.4	-19	20	-4.2	-20	18	-4.3	-19.5	19
16/01/1995	-2.8	-11	12	-2.8	-12	10	-2.8	-11.5	11
26/01/1995	-12.1	-89	152	-11.7	-85	150	-11.9	-87.2	151
7/3/1995	-6.8	-43	119	-6.4	-40	109	-6.6	-41.5	114
13/3/1995	-7.5	-44	NA	-7.8	-45	NA	-7.7	-44.5	NA
24/3/1995	-5.8	-22	NA	-5.5	-19	NA	-5.7	-20.5	NA
18/5/1995				-6.4	-42	34	-6.4	-42.0	34
22/6/1995	-8.6	-62	14	-8.6	-57	14	-8.6	-59.5	14
<u>WVolume weighted mean and total rainfall</u>	-8.2	-54.2	650	-8.2	-56.2	691	-8.3	-55.2	689

Formatted

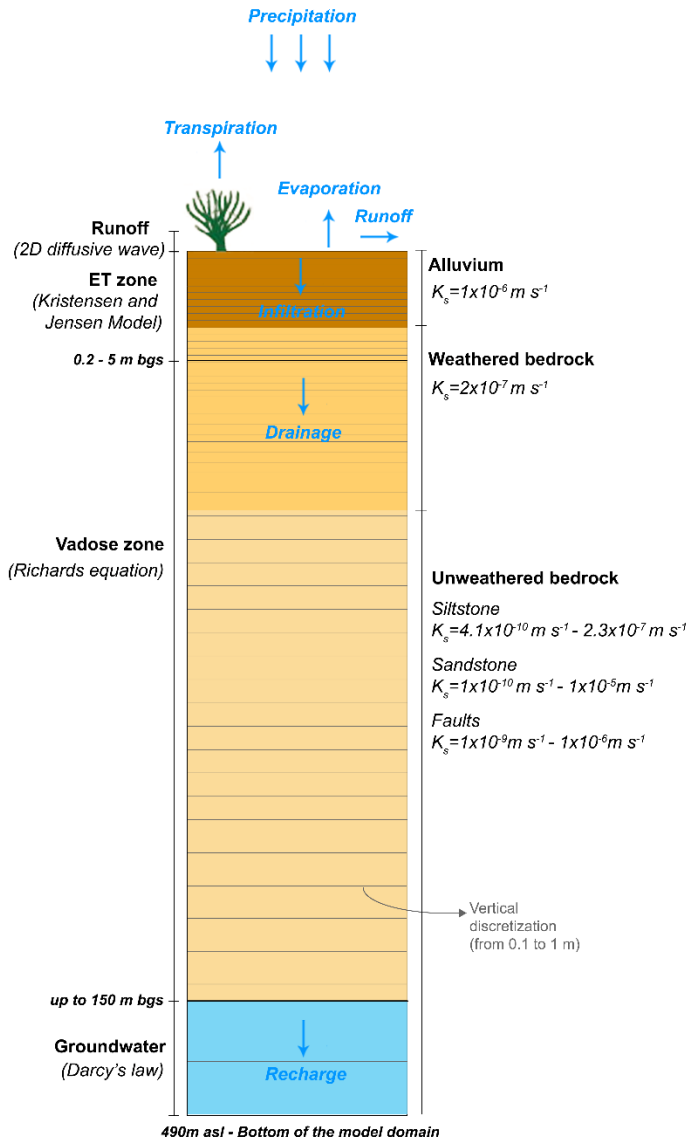
949

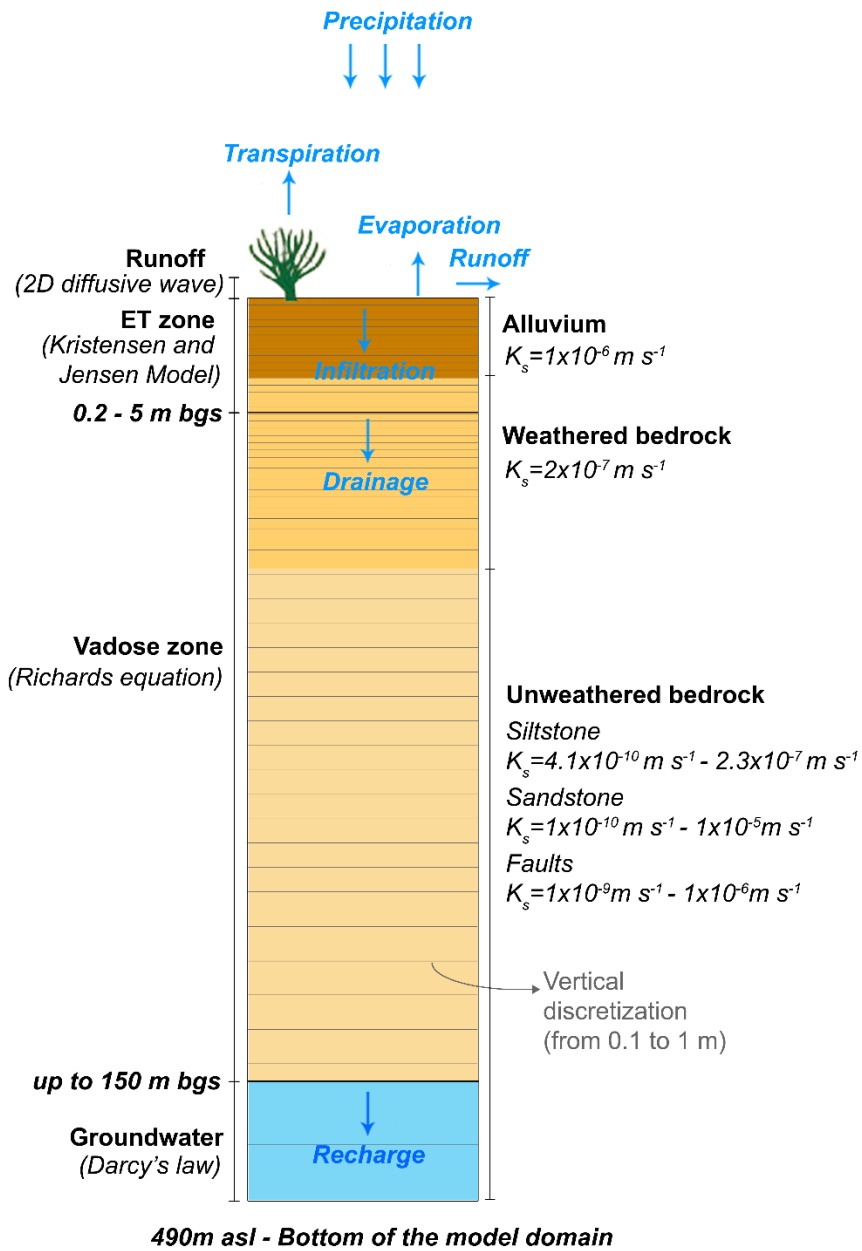


950



951 Figure 2 Geologic map of the study area and location of the wells used for calibration (blue), water isotopes sampling (red).
952 In black the two cells where unsaturated zone water budgets were analyzed.

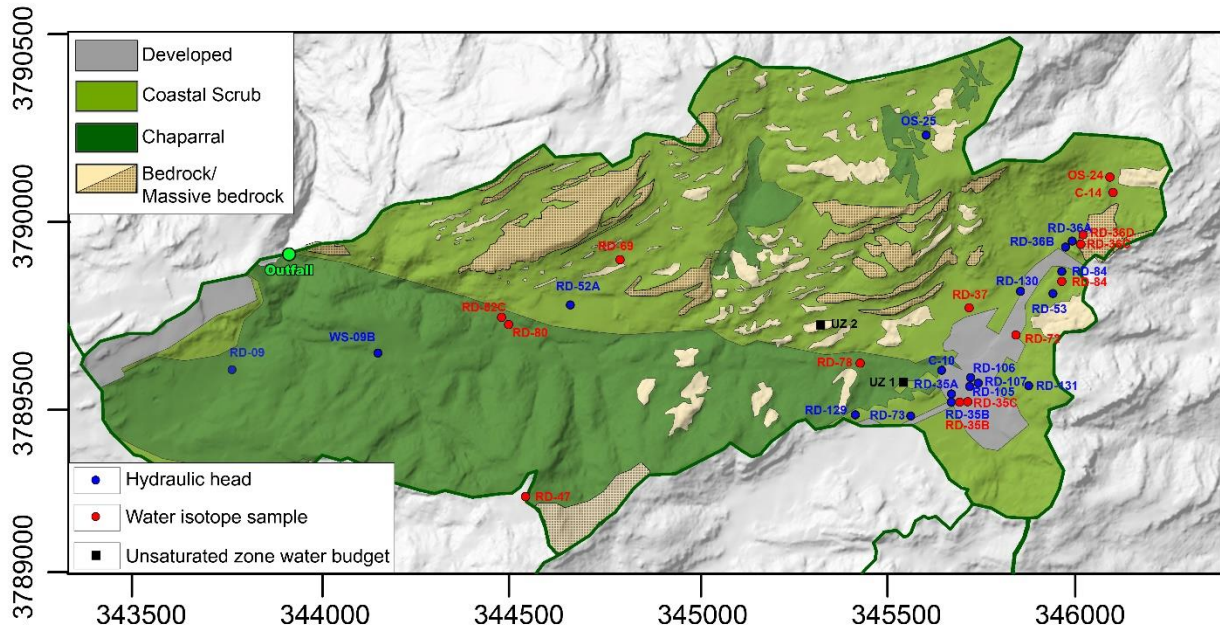




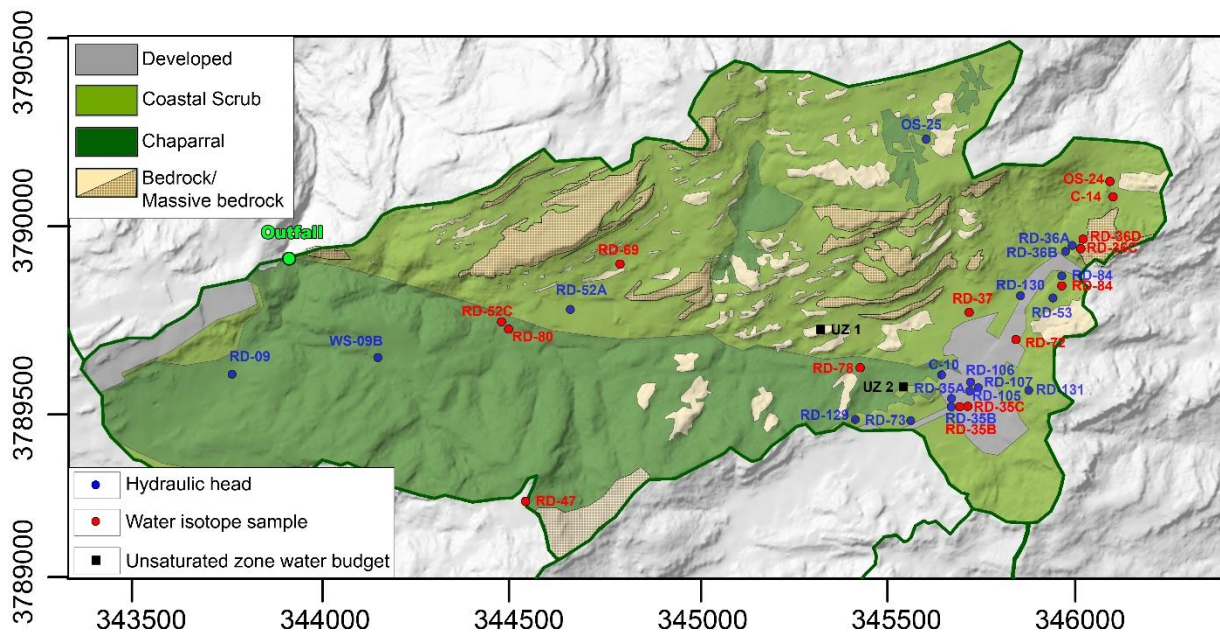
954

955 Figure 3 Description of the vertical MIKE SHE model domain

956



957

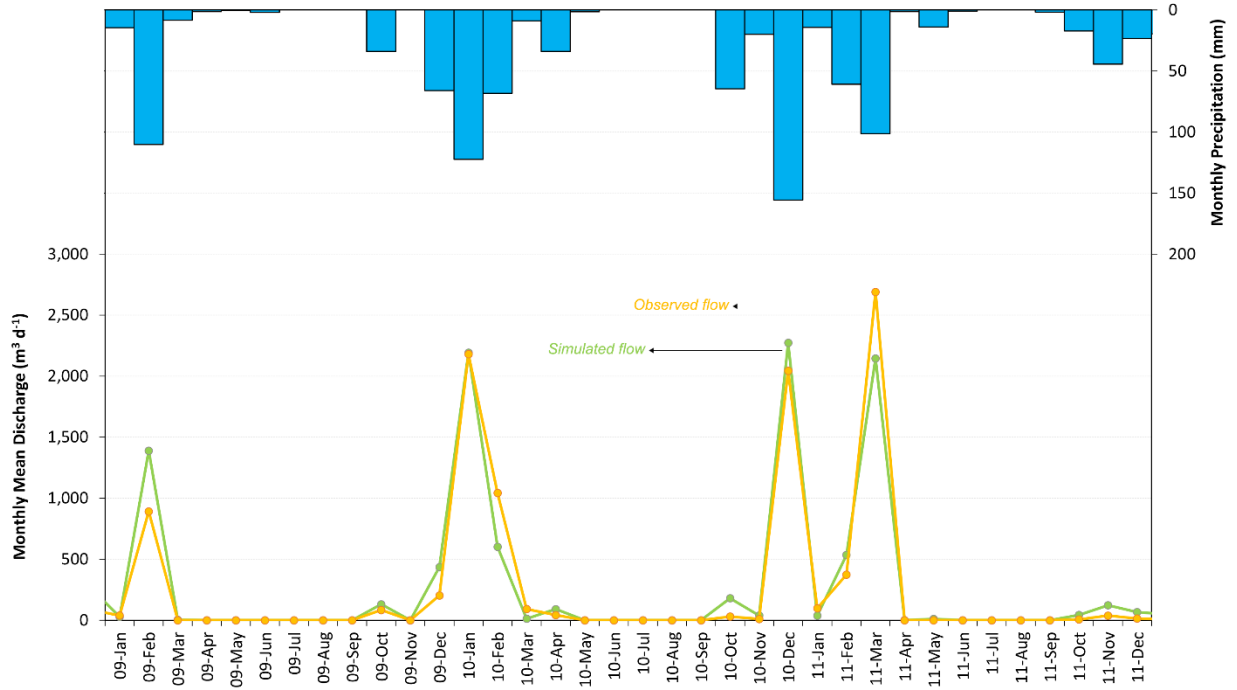


958

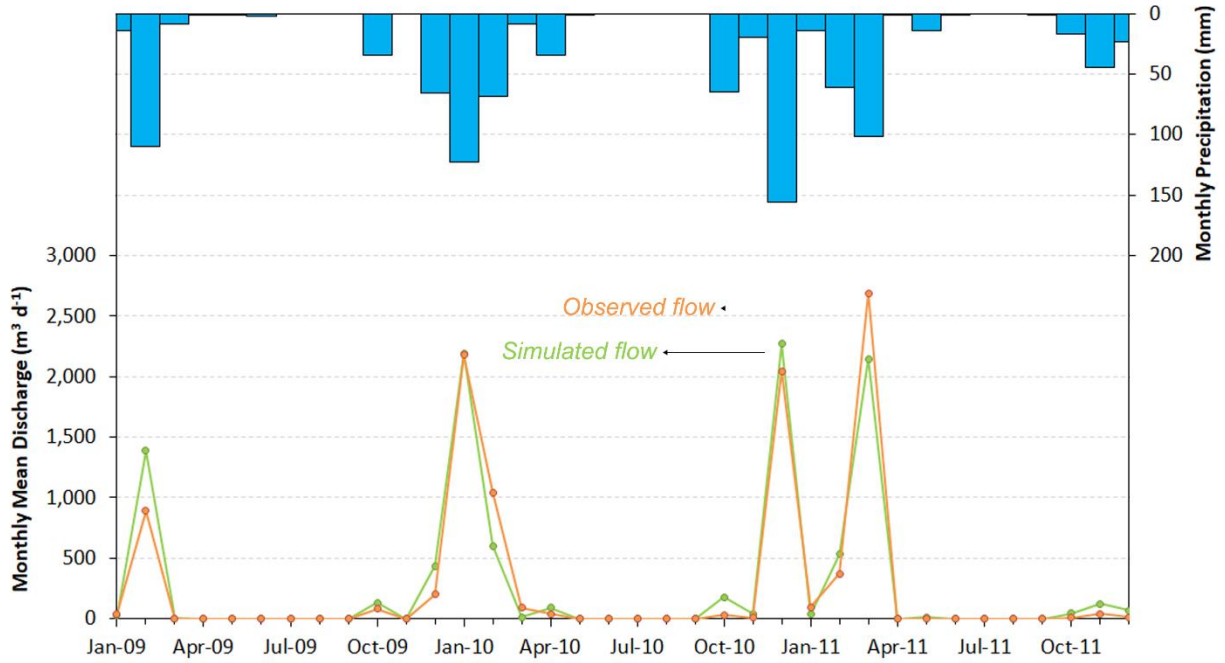
959

Figure 4 Land use map and location of the wells used for calibration (blue), water isotopes sampling (red). In black the two cells where unsaturated zone water budgets were analyzed.

960

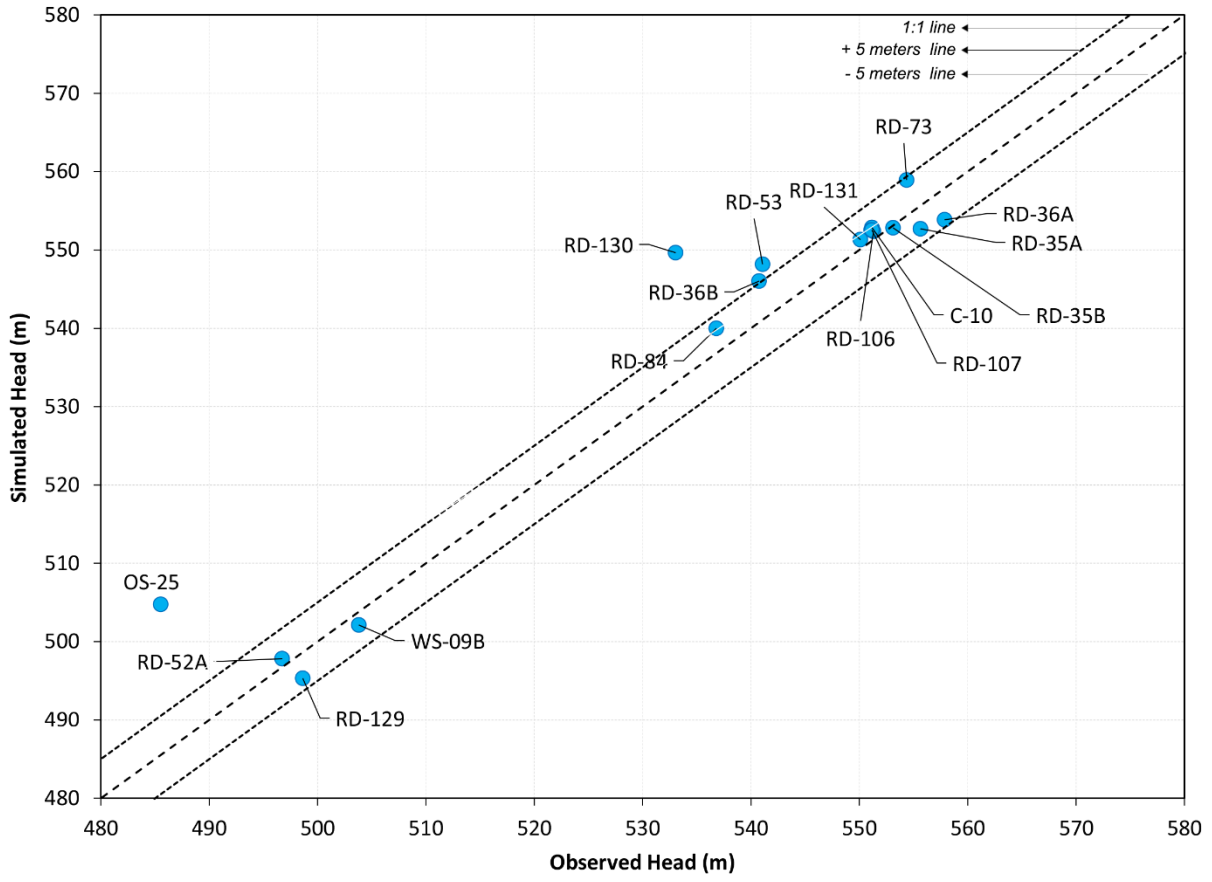


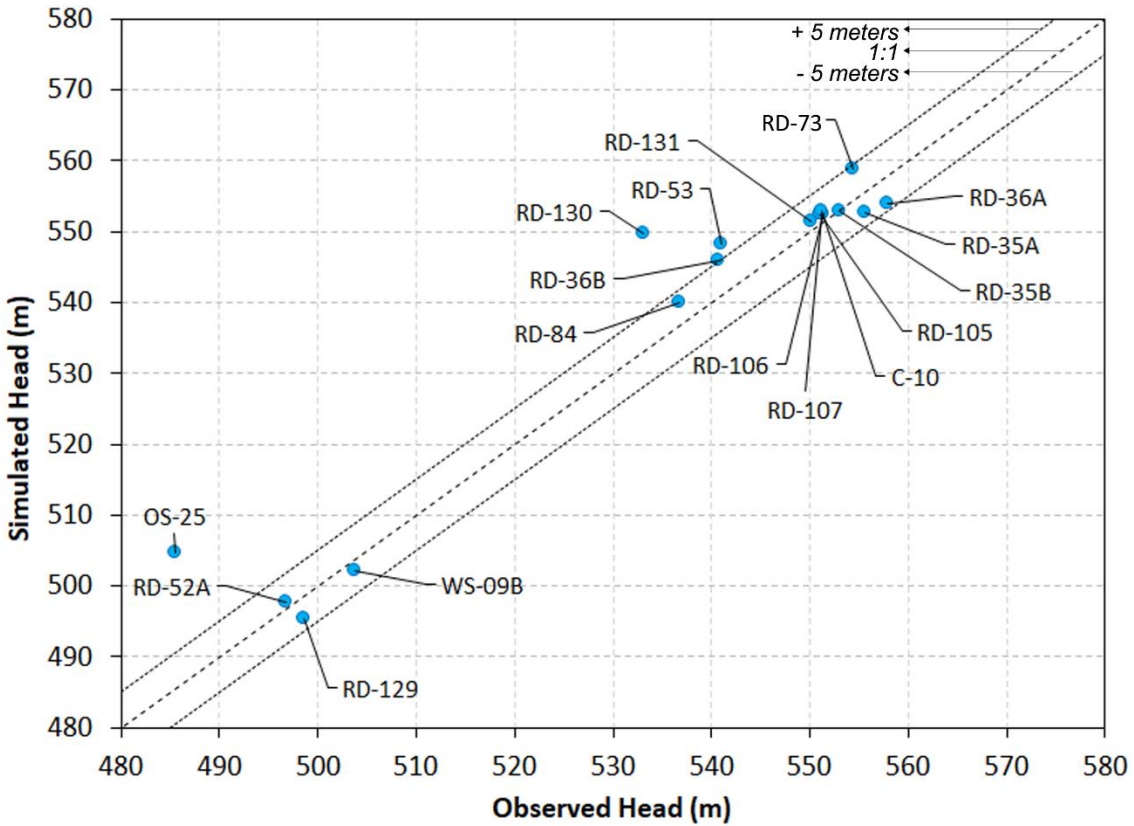
961



962
963

Figure 5 Monthly precipitation values and comparison between simulated (green) and observed (red) runoff flow at the outfall of the catchment from January 2009 to December 2011.

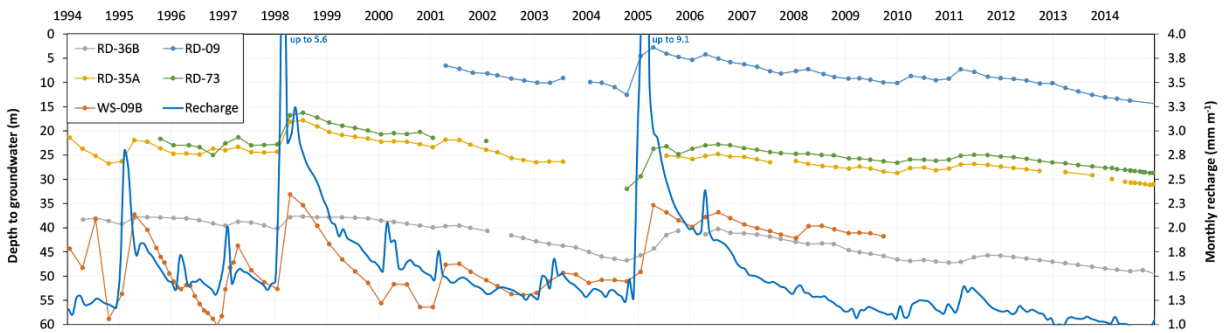




965

966 *Figure 6 Comparison between simulated and observed groundwater head data for the 17 wells.*

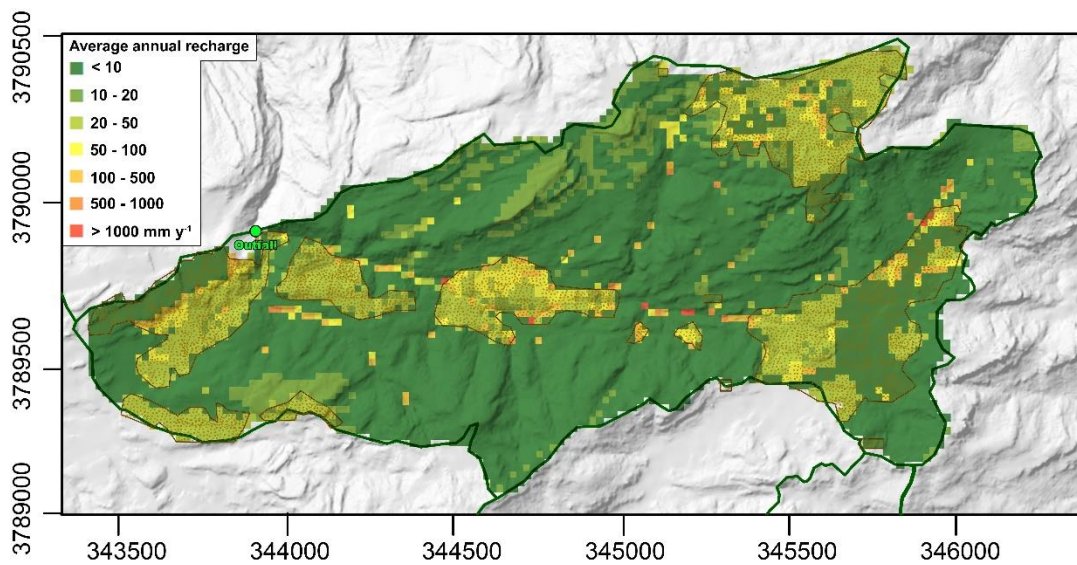
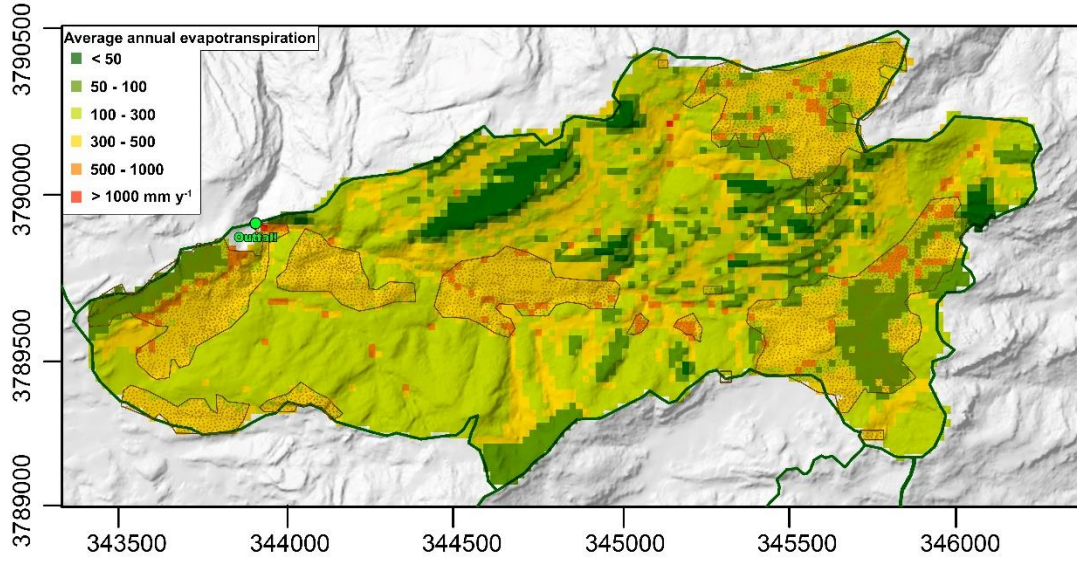
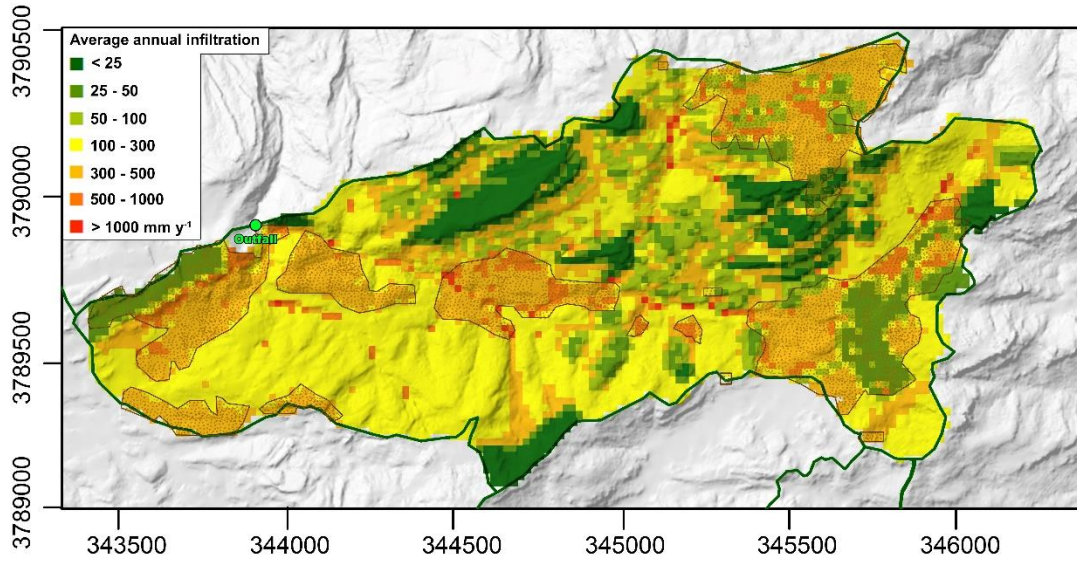
967

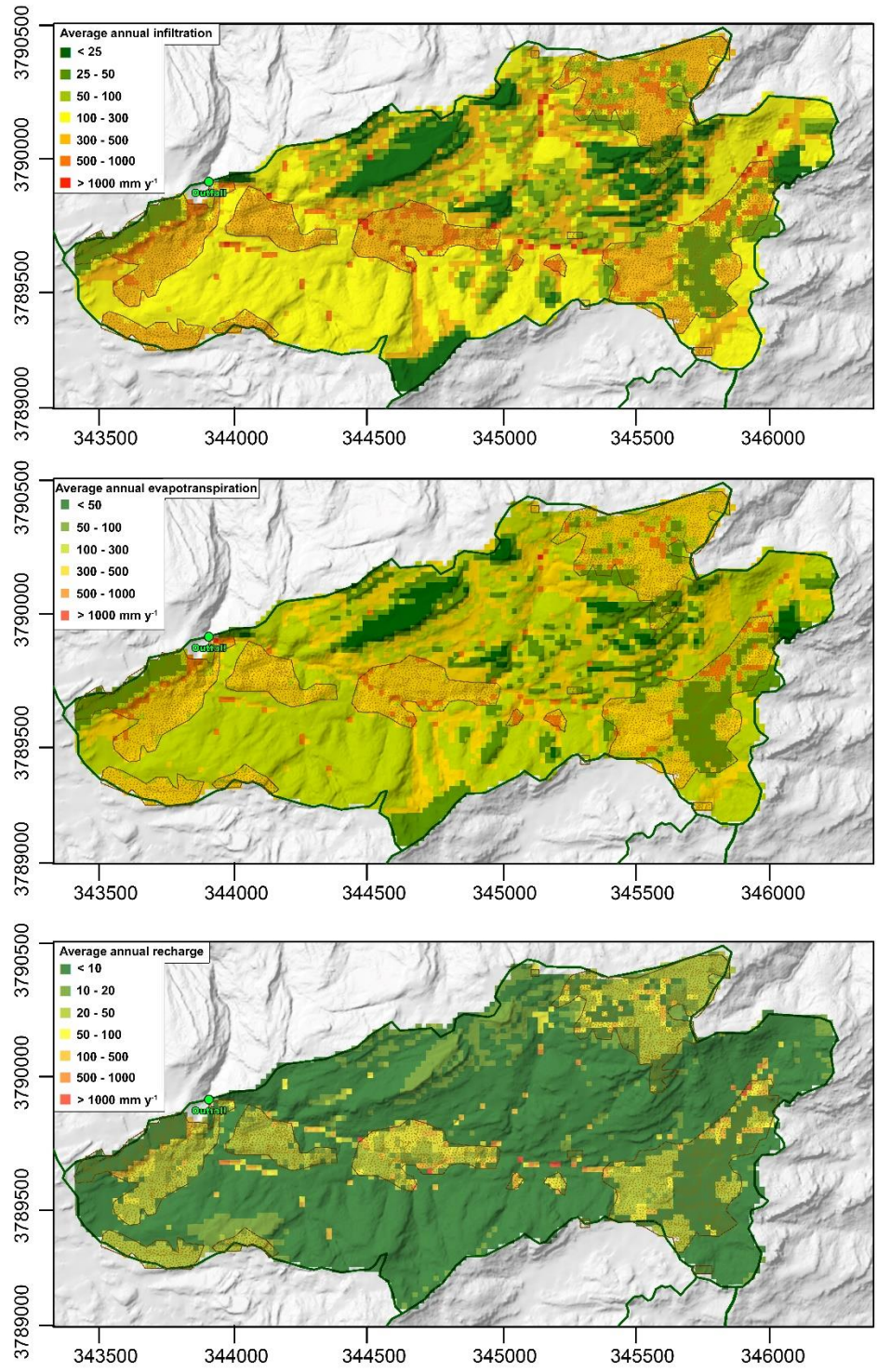


968

969 *Figure 7 Comparison between the monthly recharge time series and the depth to groundwater at five locations across the*
 970 *catchment.*

971



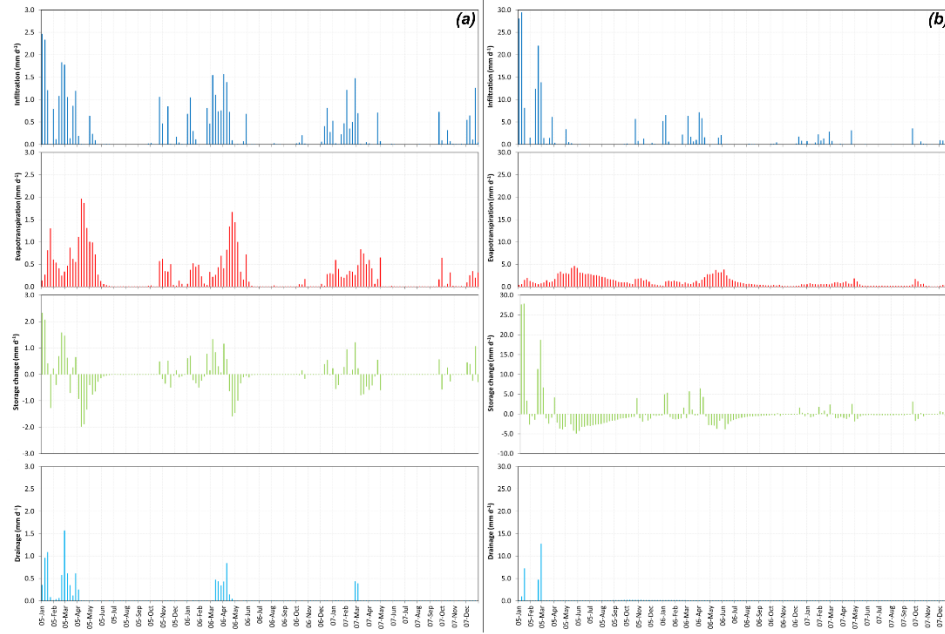


973

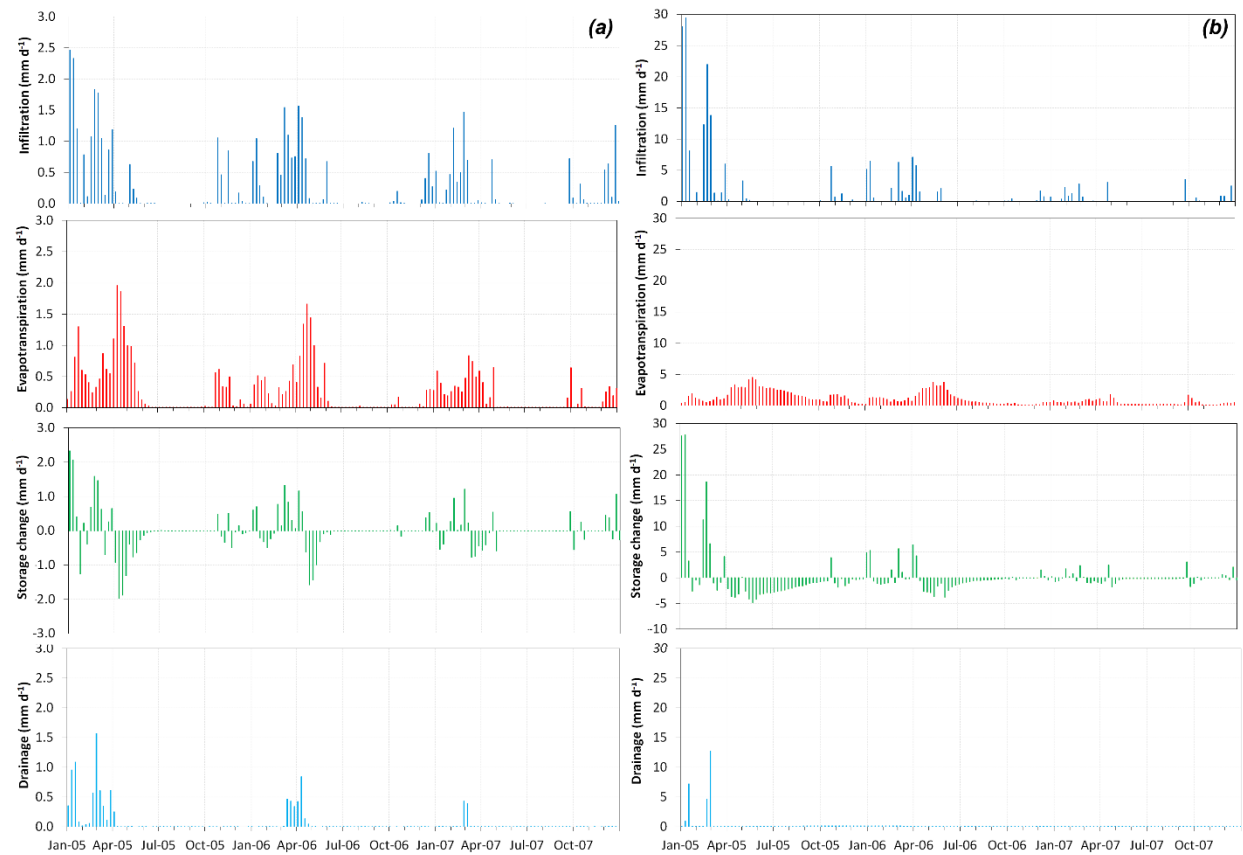
974
975

Figure 8Z. Distribution of average annual infiltration (a), evapotranspiration (b) and recharge (c). Dashed polygons represent areas with alluvium at the surface.

976



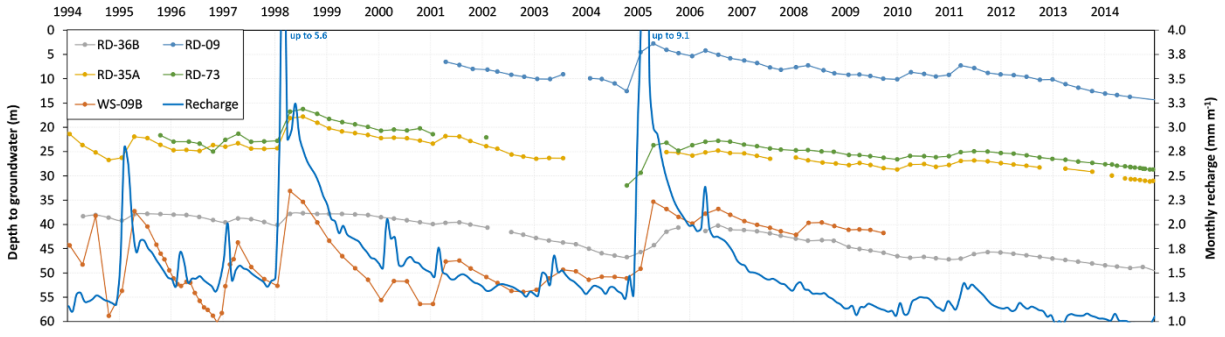
977



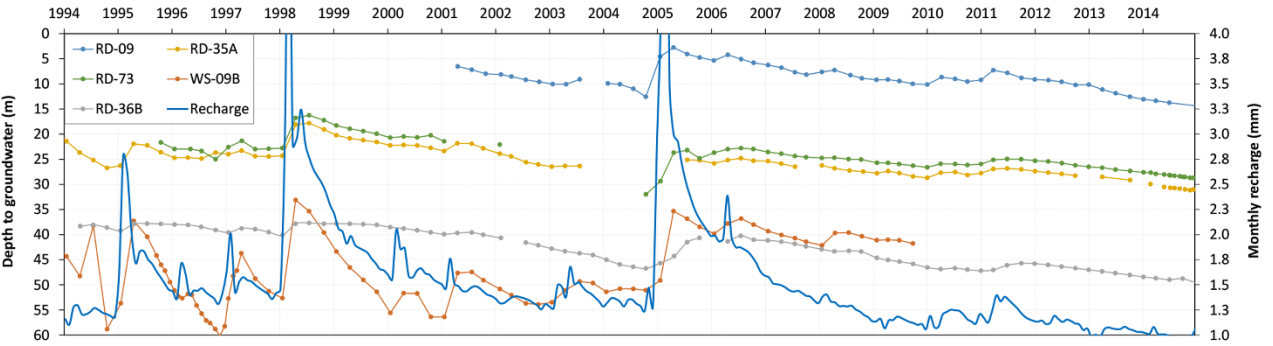
978
979
980

Figure 9-8 Unsaturated zone water budget for ET zone from January 2004 to December 2007 for two cells representative of the domain: (a) UZ-1 area with outcropping bedrock without vegetation; (b) UZ-2 area with alluvium deposit covered by vegetation.

981



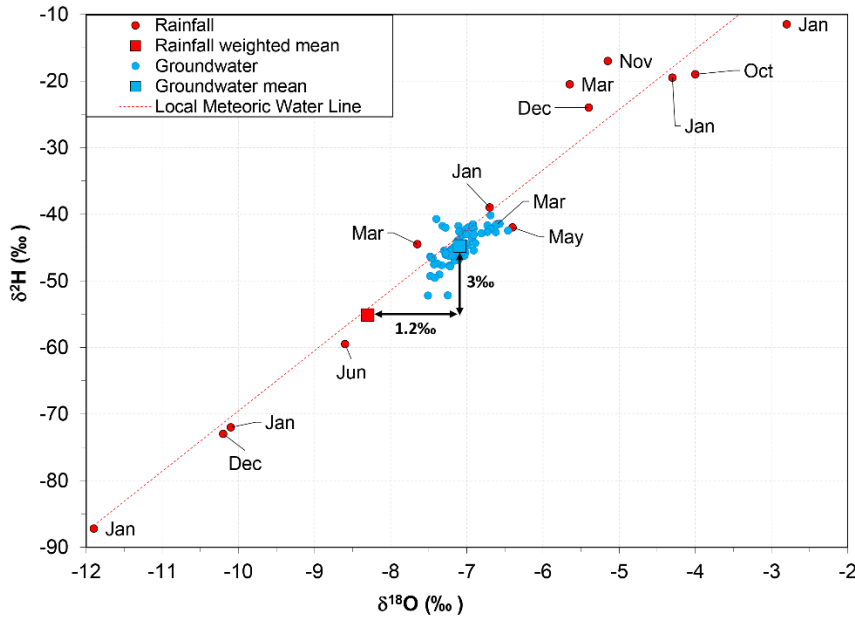
982



983

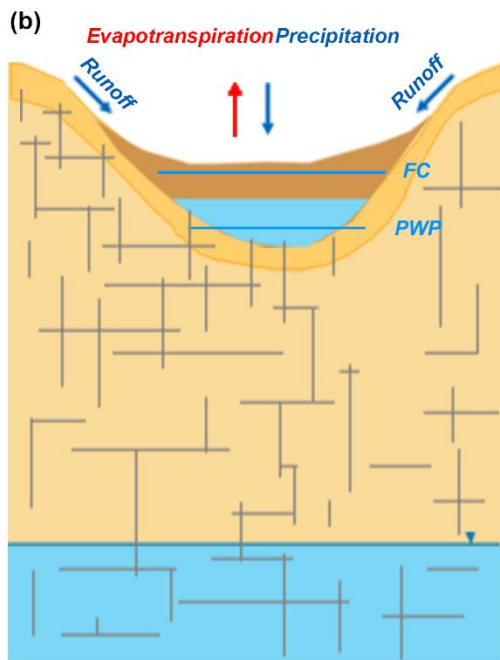
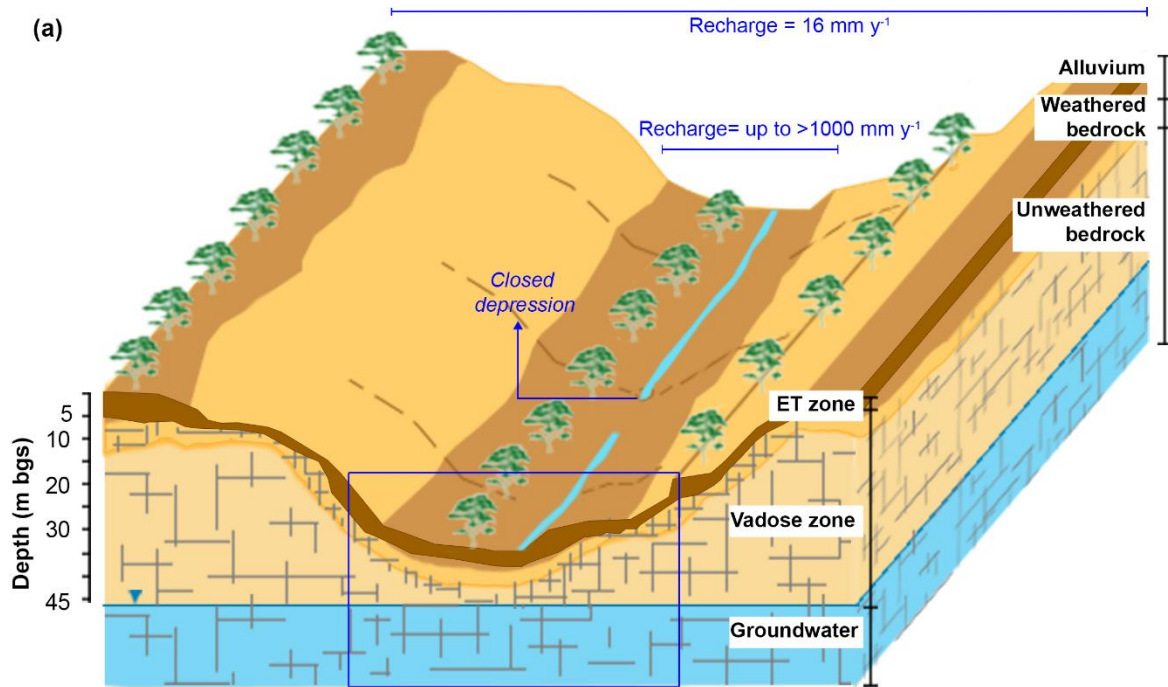
984 Figure 79 Comparison between the monthly recharge time series and the depth to groundwater at five locations across the
985 catchment.

986

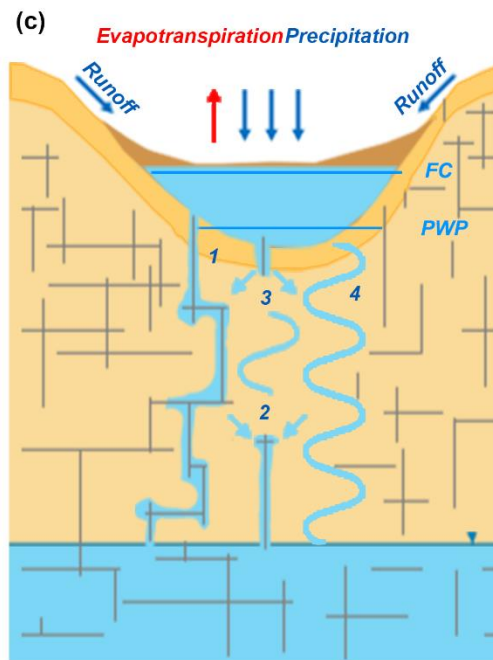


987

988 Figure 10 Water isotopes plot for rainfall samples collected at two rain gauge stations and groundwater samples from 16
989 wells of the catchment.



Dry season



Wet season

990

991 *Figure 11 Conceptual model for recharge at the site. (a) Spatial 3-D conceptual model of the catchment showing where high*
 992 *recharge occurs. 2-D schematic of the unsaturated zone hydrologic process during (b) dry season and (c) wet season. During*
 993 *the dry season water content is between the field capacity (FC) and the permanent wilting point (PWP) and therefore is*
 994 *consumed by evapotranspiration. Conversely, during the wet season, water content is above the FC and seeps into the*
 995 *underlying bedrock. Numbers describe mechanisms of flow in the vadose zone: 1 is fracture flow; 2 is water flowing from*
 996 *matrix into fractures; 3 is water flux from fractures into matrix; 4 is intergranular matrix flow.*

997